Summer 8-19-2022

3D Computer Modeling Offers New Insights Into Diatom Ecology

Joseph Mohan
University of Maine, joseph.mohan@maine.edu

3D COMPUTER MODELING OFFERS NEW INSIGHTS INTO DIATOM ECOLOGY

By

Joseph Eric Mohan

B.S. Central Michigan University, 2014

M.S. Indiana State University, 2017

A DISSERTATION

Submitted in Partial Fulfillment of the

Requirements for the Degree of

Doctor of Philosophy

(in Ecology and Environmental Science)

The Graduate School

The University of Maine

May 2022

Advisory Committee:

Jasmine Saros, Professor of Paleolimnology and Lake Ecology, Advisor

Hamish Greig, Associate Professor of Stream Ecology

Amanda Klemmer, Assistant Professor of Landscape Ecology

Kirk Maasch, Professor of Earth and Climate Sciences

Jeffery Stone, Professor of Earth and Environmental Systems

3D COMPUTER MODELING OFFERS NEW INSIGHTS INTO DIATOM ECOLOGY

By Joseph Mohan

Dissertation Advisor: Dr. Jasmine Saros

An Abstract of the Dissertation Presented
in Partial Fulfillment of the Requirements for the
Degree of Doctor of Philosophy
(in Ecology and Environmental Science)
May 2022

Algae supply over half of the Earth's global primary production and form the base of almost all aquatic food networks. Thus, changes in algal productivity or composition will induce profound shifts in many ecosystems. This research is guided by two questions. Herein I ask if 3D models of algae can be created accurately enough to use for research applications? If they can be accurately created, then how can these models be used to advance our understanding of functional trait evolution and paleoecology?

Herein, I develop 3D computer models for estimating the volume of individual algae and their parts. I also examine pressures that influence algae biomass, resource requirements, and trait evolution. Further, I apply these to an annually resolved sediment records to reveal paleontological applications that can be used to reconstruct past ecosystems and evolutionary events. This dissertation provides the means improve historical ecological reconstructions, advance predictions of ecological changes that will occur under global climate change and allow for evolutionary cost benefit analysis of traits of microscopic organisms.

For this study I exploit the sedimentary record from Herd Lake Idaho USA (44.089428, -114.173921). because it contains large (~0.5 cm) annual layers. These layers are extraordinarily

abundant in the remains of the diatom *Stephanodiscus niagarae.* These qualities present an ideal setting to produce accurate 3D computer models of a diatom that influences a large portion of the nutrient cycles in an aquatic system. The abundance of individuals provides ample data and diversity for strong statistical interpretations of the diatom populations while the annual resolution of the sediment provides a means to compare the novel methods to weather and climate data that inform us of the ecological significance of these new methods. The bounds of this study are within the years 1927 – 2011 and pertain to aquatic environments on Earth. Although these works are constrained to the recent past and local ecosystems, future applications are bound only by the geological time frame in which algae have existed and are limited in space to wherever algae are found in the universe.

DEDICATION

Everything is for my wife, my lotus ❁, and to generations yet born. You show me the way. May you inherit a habitable planet. Also for Philip Vincent Mohan II, if heaven exists I'll get that handshake when I get there.

ACKNOWLEDGEMENTS

Nanos gigantium humeris insidentes “we are but dwarves standing on the shoulders of giants” – Bernard of Chartres

I express deep gratitude and thanks to the following individuals for their time, knowledge, guidance, and contributions to this dissertation and my development as a scientist. My wife Elizabeth Whalen for endless support. My parents Bob and Michele Mohan for raising me to find the answers for myself and perpetuating my curiosity. My grandfather Philip Vincent Mohan II for inspiration and vision. To my committee for their guidance and insight. To colleagues, lab mates, contributors, mentors, and mentees, Dr. Jasmine Saros, Dr. Jeffery Stone, Dr. Reed Wicander, Dr. Hamish Greig, Dr. Amanda Klemmer, Dr. Kirk Maasch, Dr. Mark Shapley, Dr. Bruce Finney, Dr. Mark Edlund, Dr. Ed Theriot, Dr. Sarah Spaulding, Dr. Jen Latimer, Dr. Brian McGill, Dr. Brian Olsen, Dr. Zach Wood, Dr. Rachel Fowler, Dr. Jeffery Auger, Dr. Ben Burpee, Dr. Sabrina Brown, Dr. Peter Koons, Dr. Isaac Shepard, Andrea Nurse, Bethany Kile, Helena Bierly, Mitchel Paisker, and everyone that influenced my path.

Funding for this project was provided by the Gokcen Fund, the Graduate Student Government at the University of Maine, the Geological Society of America, the Churchill Exploration Fund, the Sawyer Water Research Laboratory, the School of Biology and Ecology, and the Climate Change Institute at the University of Maine.

TABLE OF CONTENTS

DEDICATION iii

ACKNOWLEDGEMENTS iv

LIST OF TABLES vii

LIST OF FIGURES viii

CHAPTER 1 INTRODUCING PHYTOPLANKTON IN THE COMPUTER REALM 1

CHAPTER 2 ON THE MATTER OF PHYTOPLANKTON: A NOVEL METHOD USING 3D COMPUTER MODELS TO CALCULATE BIOVOLUME OF MICROORGANISMS 3

Introduction 3

Materials & Procedure 8

Assessment 10

Discussion 15

Comments and recommendations 18

Acknowledgements 18

CHAPTER 3 THE ENGINEER'S APPROACH TO EVOLUTIONARY ECOLOGY: MODELING TO ASSESS TRAIT FUNCTION EFFECTS ON SELECTIVE PRESSURE WITHOUT THE CONFOUNDING INFLUENCE OF CORRELATED TRAITS 21

Introduction 21

Methods 24

Results 29

Discussion 34

Conclusions 40

CHAPTER 4 ASSESSING THE CLIMATE, WEATHER, AND NUTRIENT INTERACTIONS ON SILICA BURIAL AND SIZE STRUCTURE OF DIATOM POPULATIONS 41

Introduction 41

Methods 43

Results 48

Discussion 53

Conclusions 58

CHAPTER 5 CONCLUSIONS 60

REFERENCES 65

APPENDIX 67

BIOGRAPHY 72

LIST OF TABLES

Table 2.1 14

Table 2.2 17

Table 3.1 26

Table 3.2 32

Table 4.1 50

Table A.1..... 70

LIST OF FIGURES

Figure 2.1 7

Figure 2.2 10

Figure 2.3 12

Figure 2.4 13

Figure 3.1 23

Figure 3.2 28

Figure 3.3 30

Figure 3.4 32

Figure 3.5 33

Figure 3.6 34

Figure 4.1 46

Figure 4.2 48

Figure 4.3 49

Figure A.1 68

CHAPTER 1 INTRODUCING PHYTOPLANKTON IN THE COMPUTER REALM

Algae account for much of Earth's primary productivity and form the trophic base for nearly all aquatic systems. They regulate climate via carbon sequestration and play roles in global nutrient cycles. As such, our models for predicting ecological changes under climate change must ensure accurate estimates of these foundational groups. Yet, consensus about trends in global algal productivity, biovolume, and mass flux remains to be achieved, especially in regards to phytoplankton (Boyce *et al.* 2010; McQuatters-Gollop *et al.* 2011). Herein I surmount an effort to expose and fill in some of the gaps that are leading to unresolved ecological modeling of phytoplankton. I also offer a novel approach to trait function analysis on phytoplankton that reveal cost and benefit of traits that modify phytoplankton sinking behavior. Further, I reveal ecological drivers of phytoplankton based on functional traits and offer guidance for integrating these novel methods into paleontological studies.

What is the volume of a phytoplankton? A question that has eluded ecologists thus far. Attempts have been made to approximate the biovolume of many plankton (Hillebrand *et al.* 1999; Sun & Liu 2003) but rely on unsatisfactory simplistic models to estimate biovolume. These attempts also lump together hard outer shell that many groups of phytoplankton produce with the internal volume. Accurate biovolume models on the microscale are essential for estimating global biomass and primary production and influence on global biogeochemical cycles. I build and test 3D Computer models of a diatom population to reveal more accurate biovolume estimates and parse out the volume into the hard outer shell and inner cytoplasm components. This chapter has been published in *Limnology & Oceanography: Methods*.

Once accurate 3D models of diatoms are constructed, I ask what else are these useful for? Because 3D models can be manipulated easily to change the morphology of a diatom, I use them

in experimental simulations to test trait functions. Removing or modifying frustule (outer shell) traits has been hypothesized using gene editing in the nano-biotechnology field but specific gene to frustule editing has not yet been reached (Nymark *et al.* 2016). Because we cannot yet alter specific traits of the diatom frustule many experiments aimed at revealing trait function are confounded by correlated traits. Herein I devise simulated sinking experiments using 3D models of diatoms to test specific trait functions on sinking rates. I find that construction of spines reduces the sinking rate of a diatom and that the resource cost is greater for large diatoms and has the least effect on sinking rate.

Once the volume of the frustule has been parsed out from the total biovolume, I ask of what use is this new metric to ecological and paleontological applications. I explore the possible ecological drivers of the total silica buried by a population of diatom in a lake. Then I determine what if any influence this metric has upon the nutrient cycles in lakes and how we can use this metric for palaeoecological reconstructions. I find that the frustule or silica volume of a population of planktonic diatoms (*Stephanodiscus niagarae*) is driven by the precipitation during summer, the total phosphorus, and plays a role in Oxidizing P in lake sediments.

Herein I develop 3D models of diatoms and exhibit two lines of research that can be illuminated by this new technique. I aim to advance the fields of limnology, ecology, paleontology, and evolutionary biology with these novel methods.

CHAPTER 2 ON THE MATTER OF PHYTOPLANKTON: A NOVEL METHOD USING 3D COMPUTER MODELS TO CALCULATE BIOVOLUME OF MICROORGANISMS

Abstract

We develop a new method that allows for more accurate biovolume calculations of microorganisms. This method also allows the volume of individual skeletal features of microorganisms to be analyzed separately so that estimates of the resource cost per evolutionary adaptations may be assessed. We also provide a means to link community changes to alterations in nutrient cycles, ecosystem function, and rock-forming processes by plankton. This method integrates computer-aided design software from engineering and architecture into biological applications. Our method substantially improves the accuracy of biovolume estimates for species which currently rely upon simple geometric models that preclude the presence of ultrastructure in microorganism skeletons. In addition, using simple shapes to represent the skeletal form of microorganisms prohibits the exploration of resource cost that various adaptations, for example, spines for protection from grazers, have imposed upon plankton. Thus, integrating architectural and engineering approaches more broadly into biovolume estimations produces new insight into the physiology of microorganisms that can turn speculations into quantitative analyses.

Introduction

Biovolume is a common metric used to compare algal productivity across aquatic systems. Estimations of biovolume rely on several models to determine the amount of living matter in a parcel of water. Early biovolume estimate methods calculated values based upon simple cell counts (Kovala & Larrance 1966; Willén 1976). Paasche (1960) proposed the concept that cellular surface area controlled primary productivity in phytoplankton. The relationship

between cell volume, carbon content, and surface area is typically expressed as a regression equation for phytoplankton (Mullin *et al.* 1966). However, Strathmann (1967) pointed out that this regression equation was probably inadequate – especially regarding diatoms, which are often a major component of lake phytoplankton communities – because a large fraction of the diatom cell consists of silica dioxide, hence it would not contribute to carbon content. These studies also relied heavily on the assumption that the volume of microscopic organisms can be estimated by calculating the volume of simple shapes that reflect the general form of the organism. In the case of planktonic diatoms, for example, a cylinder is often used. Indeed similar assumptions have been used to create an extensive list of geometric shapes and the associated equations that can be used to approximate the biovolume of many phytoplankton (Hillebrand *et al.* 1999; Sun & Liu 2003).

Any method devised to estimate biovolume will have inherent limitations. The limitations of using cell counts with the approximate geometric shape to estimate biovolume are easily identifiable because organisms come in a variety of shapes and sizes. Estimates of cell sizes within phytoplankton populations can be challenging to accurately determine, particularly for diatoms or other algae with a wide range in species sizes. While using geometric models to calculate the volume of phytoplankton likely increases the accuracy substantially, the volume of many organisms is not well represented by simple shapes. Phytoplankton with complex architecture and substantial size dynamics remain problematic. As an example, planktonic diatoms generally may be approximated as cylinders but many species have undulating or broadly-domed valve faces (*e.g. Stephanodiscus, Cyclotella, Lindavia*) that can complicate reliable biovolume estimates using a cylindrical model. Sicko-Goad et al. (1984) point out that there is a lack of accuracy in measuring microscopic organisms because of irregular shapes and

complex forms. Spines, ornamentation, and other processes that protrude from the cell walls are common features of phytoplankton (Figure 2.1). Inclusion or exclusion of these features in a model representing the organism will alter the estimations of volumes that are calculated. Several groups of microorganisms produce inorganic tests, *e.g.* diatoms, radiolarians, silicoflagellates (silica dioxide), coccolithophores, foraminifera, and ostracods (calcareous). The simple models of diatoms, for example, are unable to differentiate the volume of the diatom frustule (test, made of silica dioxide) or the volume of each component that comprises the frustule (Figure 2.1).

Assessing test volume may be important in analyzing microorganisms because these parts fossilize more easily than the organic cell components. The frustules of diatoms for example are more robust than the rest of the cell and fossilize readily (Smol & Stoermer 2010). The fossil remains of diatoms contribute large quantities of biomass to aquatic sedimentary archives and in abundance can create diatomite rock formations (Harwood 2010). Diatom phytoplankton blooms can lead to increased silica burial in sediment (Figure 2.1). Silica burial in sediment often sequesters it from nutrient recycling in the water column (Conley et al. 1993). This can lead to can lead to silica depletion in aquatic systems (Schelske et al. 1986). Silica cycles are strongly intertwined with other major biogeochemical cycles and can be major controls on primary productivity in aquatic systems (Treguer and De La Rocha 2013). This species-specific method provides a means of estimating the volume of silica buried. This method will give ecologists predictive power when addressing the cascading effects that diatom community changes have on nutrient cycles.

Diatom communities and assemblages over the past century indicate pervasive species turnover driven by anthropogenic climate change and biogeochemical changes, largely through eutrophication (Wolfe *et al.* 2013). We currently lack the ability to determine the amount of

silica that is buried by individual species. Therefore, we are unable to predict how rapid changes in diatom communities may affect burial rates or nutrient pools of silica over time which can subsequently alter ecosystem functions (Figure 2.1). The next step for biovolume estimates is to build better geometric models for each species of phytoplankton.

Herein, we present a novel method for constructing accurate geometric models of microorganisms. This method aims to improve biovolume estimates of microorganisms. Our approach is to improve biovolume estimates with 3D modeling tools that can calculate volumes of architecturally complicated shapes such as found in phytoplankton, and other microscopic organisms. Specifically, we use the diatom *Stephanodiscus niagarae* as a case study to illustrate the ability of this method to improve biovolume estimates, parse out inorganic components of the organism, and determine the nutrient cost of each feature of an organism's test. We use samples recovered from the sedimentary archives from Herd Lake, Idaho to test whether this approach can help illustrate how species turnover may reflect corresponding changes in ecosystem functions. From this method we can also compare the nutrient cost of evolutionary adaptations to determine the cost-benefit relationship of the various frustule components, ornamentation, and processes.

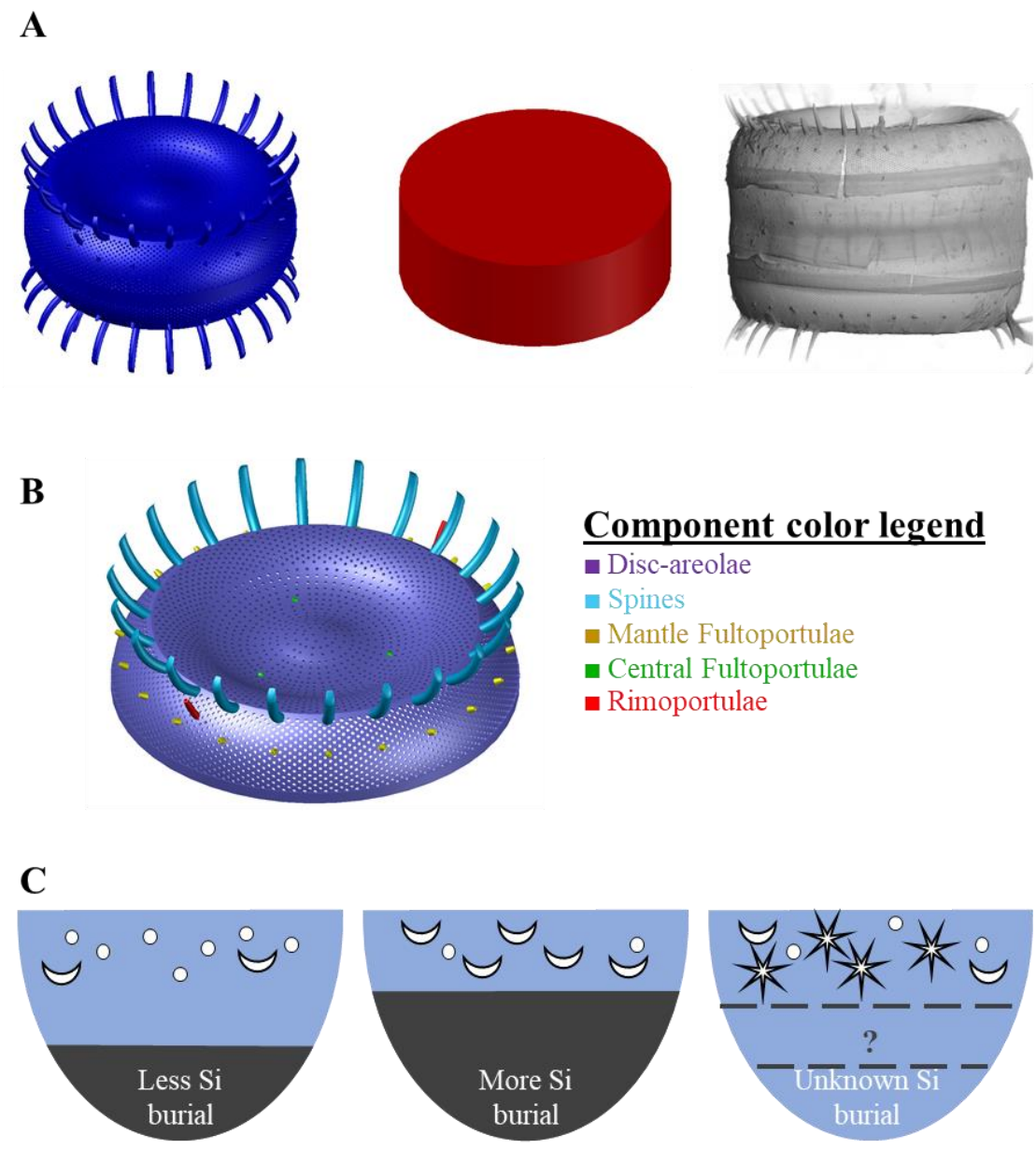

Figure 2.1 Panel A: Improved biovolume modeling. Blue model represents the method herein, red model shows the past method, and scanning electron micrograph of the diatom Stephanodiscus niagarae. Panel B: Color coded component volumes may be analyzed separately from the test. Panel C: Silica dioxide burial under different diatom hypothetical diatom communities, 3D models of the diatoms would enable prediction of how much SiO2 is buried under community changes.

Materials & Procedure

Samples used to construct these geometric models were prepared from sedimentary core samples from Herd Lake, Idaho, USA (44°05'21.9"N, 114°10'26.1"W). The Herd Lake sediments were targeted for this study because *Stephanodsicus niagarae* is one of two dominant species in the sediment for the past ~1700 years (Shapley *et al.* 2019). We used *S. niagarae* to prototype this method because it is a common species in lakes and the morphology has been studied extensively (*e.g.* Theriot and Stoermer 1984; Häkansson 2002; Theriot et al. 2006). Samples for future application could be collected from any aquatic ecosystem, (*i.e.* water column, sediment, or benthic habitat) provided they are adequately prepared for light microscopy and scanning electron microscopy. Sediment cores were collected with a Livingstone-type coring tool equipped with a "Bolivia" modification (Livingstone 1955; Myrbo & Wright 2008). Cores were transported to Idaho State University limnogeology laboratory and split (Shapley *et al.* 2019). A whole-core split was sent to Indiana State University where sub-sampling occurred. Sediment subsamples were placed in glass scintillation vials and chemically digested in 30% hydrogen peroxide in accordance with standard diatom preparation (Battarbee *et al.* 2001). Digested samples were dried on glass cover slips and affixed to microscope slides with Naphrax for light-microscope analysis. Digested samples were also dried on carbon paper affixed to aluminum stub-mounts and coated in either gold or carbon for scanning electron microscopy.

Microscopy was conducted under 1000x magnification on a Leica DM2500 light microscope, a Vega II scanning electron microscope, and a JEOL 7800F field emission scanning electron microscope. A total of 414 valves were analyzed to determine the size range of the diatom *S. niagarae* from Herd Lake. Features of the valves were counted and measured to determine the average number and size of the features according to the size of individual (supplemental).

To construct geometric models, we used computer aided design (CAD) software to create digital 3D models of diatom valves. CAD enables the user to create 3D models of complex shapes and then calculate parameters such as volume and mass of the object created. We used AutoCAD LT ® student version by Autodesk, Inc to construct the geometric models. Figure 2.2 depicts the process of creating the digital models. The cross-sectional outline of S. niagarae is created from light microscope images (Figure 2.2). Because this species is radially symmetrical, the outline was revolved around the central axis to create the diatom disc (Figure 2.2). Holes (areolae) were removed from the disc according to the proper distribution (Figure 2.2). Other structural components of the diatom valve were added such as rimoportulae (Figure 2.2), fultoportulae (Figure 2.2), and finally the spines were added (Figure 2.2) to complete the model.

Nine representative 3D models were constructed across the size range of this population of *S. niagarae* (Figure 2.3). Dimensions and component numbers were provided from morphometric analysis of *S. niagarae* (supplemental). We use the AutoCAD command MASSPROP which calculates and exhibits the mass and volume properties of the 3D solid object. The volume of silica dioxide for each 3D solid in the suite of nine representative models is shown in Figure 2.3. The representative models are then fit with a regression model that yields a mathematical formula for finding the volume of silica in *S. niagarae* based on the diameter size range of the species (Figure 2.3). For each representative valve, biovolume is calculated by replicating the valve across a mirrored plane. Adding the internal shape volume to the two valves that make up the cell gives the biovolume of each model as in Figure 2.1.

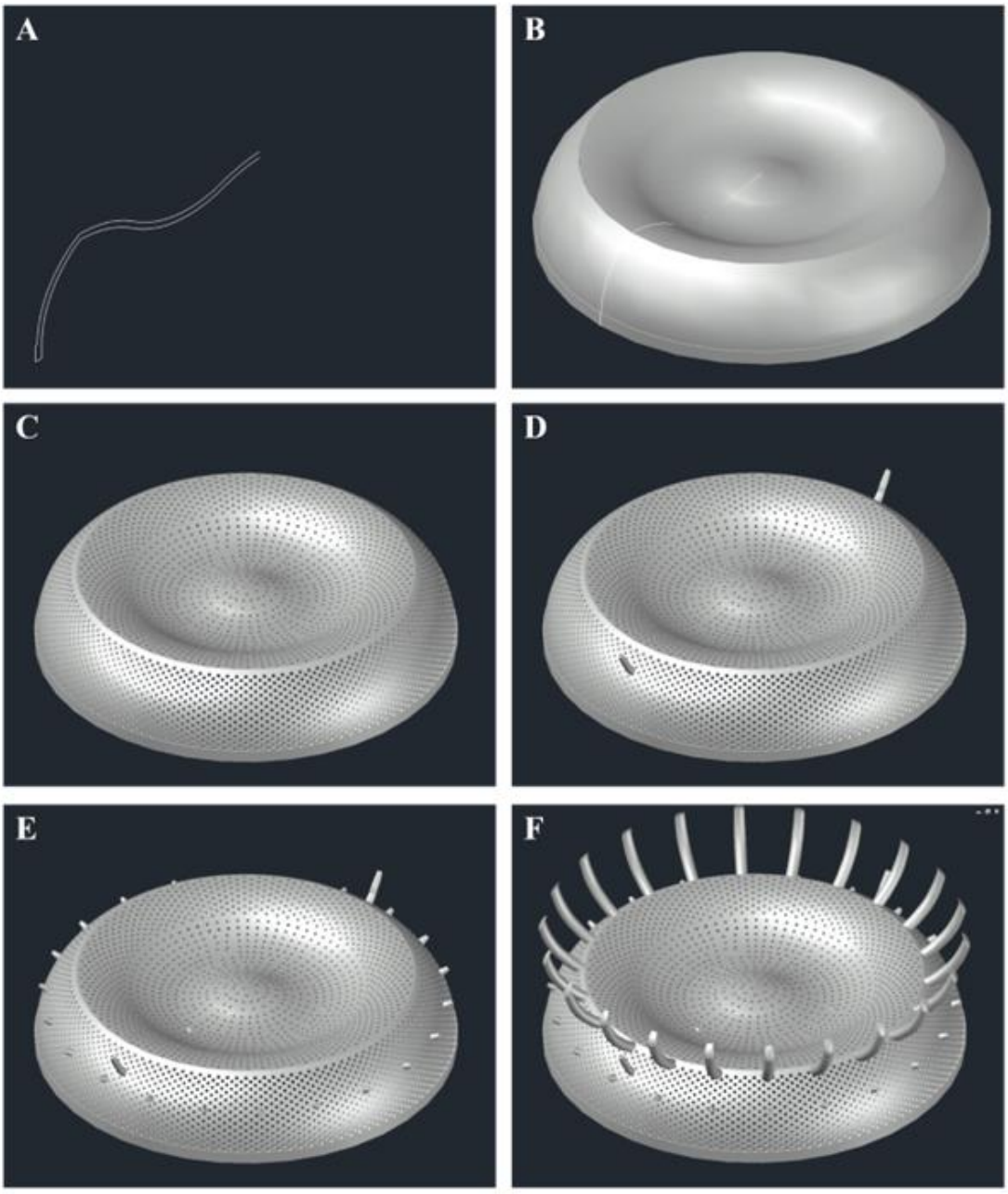

Figure 2.2 Conceptual diagram of the AutoCAD 3D modeling process. The valve outline is constructed from mantle view LM images (A). The outline is revolved around the Z axis about the central point to construct a 3D disc (B). Areolae are arranged in fascicles and removed from the discoid (C). Rimoportulae are added (D). Fultoportulae are added (E). The model is complete with the addition of Spines (F).

Assessment

Use of CAD technology in reconstructing accurate computer models of objects is a well established practice in engineering and architectural applications. Typical uses include reconstructing civil infrastructure of buildings (Fathi & Lourakis 2015; Steilein 1996). We utilize the established methods of building reconstruction to create 3D reconstructions of microscopic organisms. Assessments of our models are made by comparing our calculated biovolume results to the results of past methods. We compare our biovolume results those of seven other biovolume calculations of *S. niagarae* and similarly sized *Stephanodiscus* from past studies (Table 2.1 & Figure 2.4). Across the size range of *S. niagarae*, we calculated a biovolume range from 9,900 – 88,000 μm^3. Other calculations of biovolume of *S. niagarae* range from 12,000 – 111,000 μm^3 for the same size range (Sun & Liu 2003). Sicko-Goad et al. (1984) calculated a biovolume of 21,000 μm^3 and valve volume of 1,260 μm^3. The biovolume calculated by Sicko-Goad *et al.* (1984) is based upon dry weight averages divided by number of individuals in the population which yields a single average biovolume for the population rather than a range of biovolumes associated with the size range for the population. Still, these average values are within the range calculated herein. Comparison of biovolumes from similar taxa also indicate similar biovolume ranges (Table 2.1 & Figure 2.4).

Calculations based on simple geometric models (Hillebrand *et al.* 1999; Sun & Liu 2003) overestimate biovolume for *S. niagarae* by 17.5% – 20.7% when compared to the method described herein. Differences between methods arise because approximating cell structure with a cylinder does not account for the intricate architectural nature of biological organisms. Specifically, the inclusion of space that the diatom does not occupy due to undulating surfaces and spines inflates the apparent diameter. The fundamental flaw in simple geometric models is that organisms are rarely ever simple shapes. Diatoms like *S. niagarae* and other circular species

are not exactly cylinders. They are made up of many complex shapes with bulging outlines and undulations that are not well represented by simple shapes. Our model organisms, *S. niagarae*, is ornamented with long spines and other features such as fultoportulae and rimoportula that extend out from the main body of the cell.

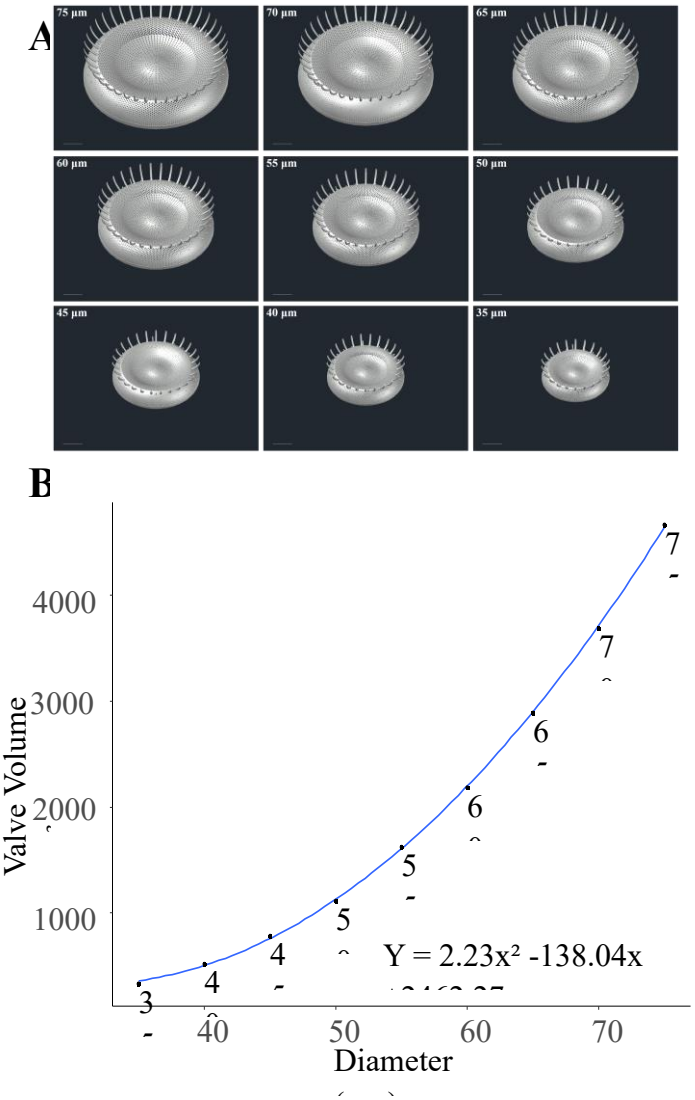

Figure 2.3 Panel A: Nine representative 3D CAD models of S. niagarae across the size range of the population found in the study population. Panels labeled by the diameter of the model. Scale bars are all 10 µm. Panel B: Calculated valve volumes based on a suite of nine CAD models across the size range of S. niagarae. Mathematical model shown in blue used to find the formula exhibited below.

Figure 2.4 Panel A: Graphic comparison of biovolume calculated herein vs. Sun et al's (2003) method. Panel B: Bar plot comparing the biovolume of S. niagarae and similar taxa, data represented is given in Table 2.1. *Single values from Table 2.1.

Limitations of this method are a steeper learning curve and longer time to implement the method when compared to the simple geometric model method. The method described herein relies upon operator skills in construction of the 3D model and skill in working in 3D modeling software such as AutoCAD. For species that do not have a model created this is a time-consuming process. The amount of time required to create a model is difficult to estimate because it depends upon many factors *e.g.* user proficiency with software, abundance of organisms, architectural complexity of traits on the organism, number of traits and structures that comprise the organism, *etc.* This species took about three months to complete from start of data collection to final model. However, for existing models the time and skills required to calculate the biovolume of an individual are reduced to the arithmetic skills required of previous methods described above. The hurdle of time may be overcome as new species are modeled; the creation of a database of models would overcoming this limitation. The method requires few measurements and microscopy beyond that required for proper taxonomic description and can thus be implemented for most species described and species to be described in the future.

Species	Valve Volume (µm³)	Biovolume (µm³)	Reference
S. niagarae	340 – 4,660	9,900 – 88,000	Herein
S. niagarae		12,000 – 111,000	*Sun, *et al.* 2003
S. niagarae	1,260	21,000	Sicko-Goad, *et al.* 1984
S. rotula		5,640 – 36,160	Olenina, *et al.* 2006
S. rotula		8,600	Gibson, *et al.* 1971
S. astraea		5,930 – 15,980	Reynolds, 1984
S. astraea		25,000	Einsele & Grim, 1938
Stephanodiscus sp.		~8,000 – 11,000	Reynolds, 2006

Table 2.1 Biovolume calculated herein compared to other studies reported biovolume for Stephanodiscus niagarae and Stephanodiscus with overlapping size distributions. * Indicates that the volume was calculated via the referenced method.

Discussion

The aim of this research was to construct more accurate geometric models to improve biovolume estimates of phytoplankton. We also aimed to allow for species-specific analysis of nutrient burial in sediment to improve investigations of connections between species shifts and biogeochemical ecosystem functions. We have shown that construction of species-specific 3D models is possible for phytoplankton and that this method considers the intricate architecture of biological organisms.

The ability to quantitatively measure the architecture of microscopic organisms enables us to test questions that until now could only be answered for macroscopic organisms. 3D CAD models can provide shape, weight, morphology, volume, and surface area. 3D analysis of diatom valves has been applied in bioengineering and nanotechnology studies. Diatoms are attractive candidates for the study of structural material design, light harvesting, photonics, and biosensing (Lu *et al.* 2015). Utilizing 3D modeling capabilities described herein with environmental data would clarify rates of silica burial and dissolution. This method will also enable future studies to quantify changes in silica burial as a consequence of shifts in species composition of a diatom community in ecological studies or diatom assemblages in paleontological analyses. While diatoms tend to bury silica dioxide when they sink, some portion of the frustule can be dissolved back into the water. The rate of dissolution is different per species as it depends on weight, morphology and surface area (Loucaides *et al.* 2011). As an example of resource cost of specific adaptation, we find that the spines of *S. niagarae* cost 6% – 24% of the total silica dioxide used in the valve (Table 2.2). Such a resource intensive structure must be worth the benefit gained from these anti-predation features. This seems especially true for *S. niagarae* because the smallest valves commit almost a quarter of their total silica dioxide into the spines whereas the largest commit only 6%. This method will enable evolutionary research to assess specific

resource allocation that newly evolved morphological features require. *Stephanodiscus yellowstonensis* for example evolved from *S. niagarae* rapidly in Yellowstone Lake, Montana, USA. It is marked by a drastic reduction in the number of spines and fultoportulae per frustule (Theriot *et al.* 2006; Theriot & Stoermer 1984). Using this method, a nutrient budget cost benefit analysis could be constructed to determine the reduction in silica dioxide required to create frustules of *S. yellowstonensis* versus *S. niagarae*. Further possibilities are opened in linking rock cycle processes to evolution. The genus *Stephanodiscus* is a common species found in diatomite rock formations. An evolutionary change in a species of rock forming diatom will induce a change in the rock formation process that our method can measure. This method may also be adapted to assess other taxa that have undergone morphological evolution.

This new capability can be expanded to all aquatic sciences. Diatoms are key drivers of the silica cycle (Treguer & De La Rocha 2013). Diatom diversity also controls the carbon cycle in the ocean where morphological diversity leads to carbon and silica export diversity. Heavily silicified diatoms export more nutrients to the deep ocean. This phenomenon has been discussed in general terms, *i.e.* higher or lower amounts of nutrients buried and the need for physiological studies of diatoms to determine their role in biological nutrient pumps is highlighted by Tréguer et al. (2018). When applied to other taxa, 3D modeling will allow for quantification of other biogeochemical cycles. Specifically, application of this method to coccolithophores and foraminifera would reveal links between species diversity shifts and the carbonate cycle. Applications beyond these will uncover links between species shifting and biogeochemical cycles that control ecosystem functions.

Component color legend

- Disc-areolae
- Spines
- Mantle Fultoportulae
- Central Fultoportulae
- Rimoportulae

Volume (µm³)

Diameter	Disc-areolae	Spines	Mantle Fultoportulae	Central Fultoportulae	Rimoportulae	Valve
75	4353	300	5	0.32	2.5	4662
70	3398	281	5	0.34	2.4	3688
65	2635	245	5	0.35	2.3	2889
60	1960	217	5	0.34	2.2	2185
55	1443	172	4	0.33	2.0	1623
50	973	135	4	0.30	1.9	1116
45	667	108	4	0.27	1.8	782
40	418	97	4	0.22	1.7	521
35	248	81	3	0.16	1.5	336

Volume as percent of Valve

Diameter	Disc-areolae	Spines	Mantle Fultoportulae	Central Fultoportulae	Rimoportulae
75	93	6	0.1	0.01	0.05
70	92	7	0.2	0.01	0.07
65	91	8	0.2	0.01	0.08
60	89	9	0.2	0.02	0.10
55	88	10	0.3	0.02	0.13
50	87	12	0.4	0.03	0.17
45	85	13	0.6	0.03	0.23
40	80	18	0.8	0.04	0.32
35	73	24	1.1	0.05	0.46

Table 2.2 Volume of each component of a S. niagarae. Component volume as a percent of the valve volume given for each of the nine size-representative models. Color coded model of the 35 µm is shown below to highlight each ultrastructure. Disc – areolae indicated the volume of the disc minus the areolae.

Comments and recommendations

It should be noted that this method is not intended as a bench tool for analysis. It is intended as a strong tool for improving our understanding of microscopic organisms. Applications suggested here include assessing evolutionary cost and function of ultrastructures, improving historic reconstructions, predicting ecological changes, skeletal engineering, and nanotechnology.

For this and future intended studies of *S. niagarae* it is critical that models be as accurate as possible. Future users must weight the time to accuracy cost for each application. Future users will have to decide where to take liberties in modeling based upon the questions they have and tolerance for accuracy. We accomplished this high degree of accuracy in two ways. The first is by accurate measurements of organisms under microscopic analysis and measurement of enough individuals to ensure anomalous individuals do not affect the data set. Secondly, the operator must be proficient in 3D CAD modeling. Learning CAD is primarily cognitive and motor-control related. The skill set required to create these models can be learned to proficiency in around 16 weeks (Hamade *et al.* 2007). We implement AutoCAD in this study however, many CAD software are available, and some are free to use. Preference for software type should be considered by the user based on level of proficiency and software capabilities. Sample preparation methods and procedures will need to fit the organism being analyzed. The procedures outlined herein can be easily adapted for organisms with hard outer shells.

Acknowledgements

We thank the following people and institutions. Dr. Mark Shapley for providing sediment core material, Bethany Kile for subsampling the core for diatom analysis, Helena Beirly for initial light microscopy and data acquisition, Dr. Jen Latimer for providing laboratory

equipment, the Integrated Nanosystems Development Institute at Indiana University Purdue University Indianapolis and University of Maine's Earth and Climate Science Electron Microscopy Laboratory for granting access to their scanning electron microscopes. We thank the following for funding that supported this research: the University of Maine's Graduate Student government research grants and summer writing fellowship.

CHAPTER 3 THE ENGINEER'S APPROACH TO EVOLUTIONARY ECOLOGY: MODELING TO ASSESS TRAIT FUNCTION EFFECTS ON SELECTIVE PRESSURE WITHOUT THE CONFOUNDING INFLUENCE OF CORRELATED TRAITS

Introduction

Our understanding of evolutionary ecology hinges upon empirical knowledge of natural selection. In the past few decades we have developed and refined tools for assessing phenotypic variation and evolution of quantitative traits (Kingsolver *et al.* 2001). Regardless of the genetic basis, natural selection acts upon phenotypes (Lande & Arnold 1983), resulting in great diversity in the forms of organisms.

One group of organisms with great diversity is the diatoms, which are unicellular, eukaryotic organisms. There are estimated to be well over 100,000 species of diatom, each with a uniquely shaped cell wall called the frustule (Julius & Theriot 2010). These uniquely shaped frustules exhibit many phenotypic traits that serve multiple functions and are typically correlated with the size of the diatom. Because natural selection acts upon phenotypes, diatom architecture is a highly plastic trait and can evolve rapidly (Theriot *et al.* 2006). Thus, linking trait function to selective pressure is paramount to improving our understanding of both diatom evolution and evolutionary ecology.

One major selection pressure on planktonic diatoms is gravity, leading to sinking which is a major loss process for phytoplankton. Sinking losses (sedimentation) account for between 28 to 100% of diatom population loss (Reynolds & Wiseman 1982). Many groups of phytoplankton are autotrophic and must spend a good portion of their life cycle in the light. Variation in phenotypic response to gravity varies greatly among phytoplankton but can be parsed into two major groups of adaptations, either change cell density or change cell surface area to volume

ratio. Sinking is the inevitable result of the force of gravity and can be both detrimental or advantageous for phytoplankton and diatom populations. The evolution of silica frustules may be a response to regulate density and sinking in populations (Ferris & Lehman 2007; Raven & Waite 2004).

Dissecting cause and effect relationships of diatom frustule architecture is convoluted by correlated traits. The evolution of correlated traits is a major hurdle in finding causal relationships of traits especially when many traits are genetically correlated to each other (Price & Langen 1992). Diatom architecture is flush with correlated traits, as the overall size often correlates with many traits. The diatom *Stephanodiscus niagarae* and its daughter species exhibit many well correlated traits, such as spines, rimoportulae, and fultoportulae (Figure 3.1) (Theriot *et al.* 2006; Theriot & Stoermer 1982, 1984). These correlated traits confound any observational data or laboratory experiments that investigate what influence the presence of spines may have upon sinking rates.

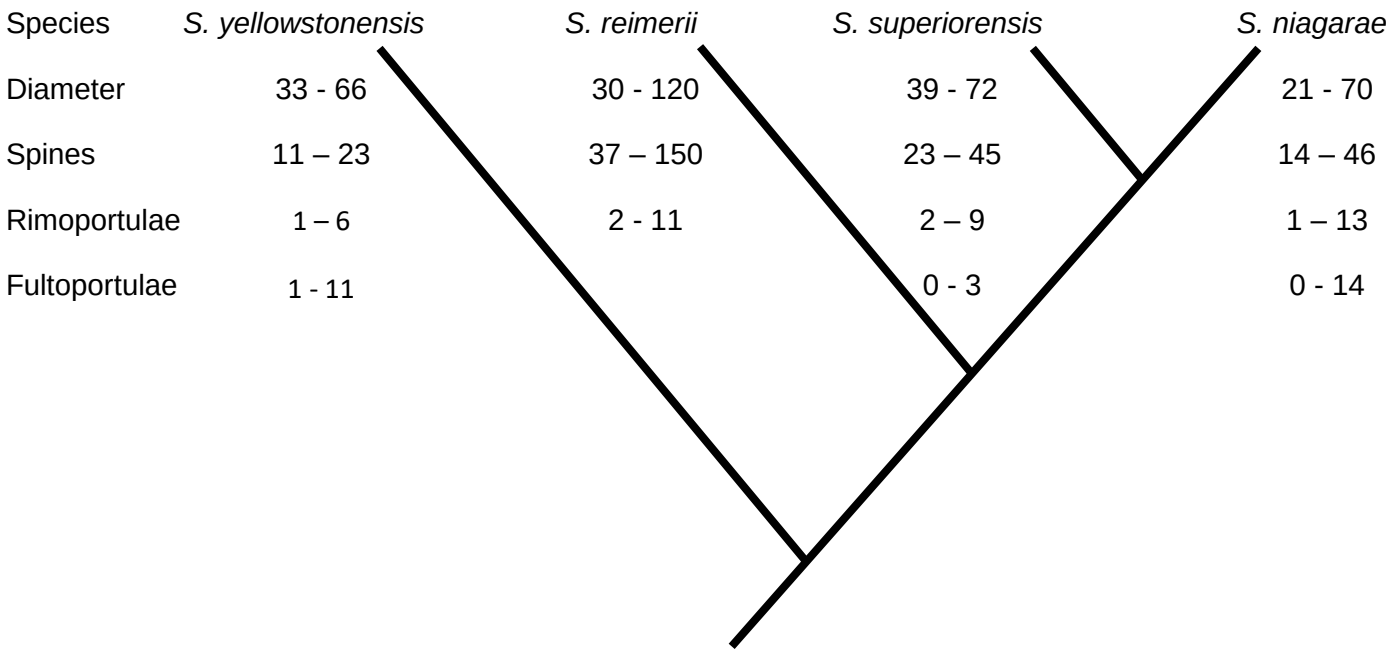

Figure 3.1: Phylogenic tree of the diatom *S. niagarae* and its daughter species. Data consolidated from Theriot *et al* (2006) and Theriot & Stoermer (1982, 1984).

Correlated traits confound experimental designs and observation of natural phenomenon aimed at assessing trait function. Correlation between traits seriously complicates the measurement of phenotypic selection because selection pressures exerted on a trait have direct and indirect effects on trait distribution of correlated traits (Lande & Arnold 1983). Correlated traits also make it difficult to infer causal relationships of trait functions from observations of natural phenomenon. Because many aspects of the phenotype are not easily manipulated in experiments, many estimates of phenotypic influences on fitness are inferred from partial regression of observational data. Regression is a method for prediction and is only able to infer unbiased estimates of causation under very limited parameters, many of which do not take into account correlated trait confounders (Walker 2014).

Our understanding of diatom evolution will expand greatly if we can devise a way to analyze sinking rates of a species with and without spines in the absence of confounding variables that arise by devising interspecies experiments. Interspecies studies contain differences in diatom morphology and are difficult to interpret the specific variation caused by spines. We cannot in natural or laboratory experiments observe or measure the direct effect that spines have upon sinking rate because spines are correlated with many other traits on the diatom frustule. We can observe differences in ecological optima across similar species (Kilham *et al.* 1996; Theriot & Stoermer 1982) however because similar species contain the same correlated traits we cannot parse out which trait is responsible for the change in ecosystem and habitat preference or optima.

Herein, we ask: 1) whether spines affect the sinking rate of plankton, 2) how this relationship varies with cell size, and 3) if spines provide a benefit against sinking, what is the resource cost of adding them? We design a way to analyze a single trait function, in this case spine influence on sinking rate in diatoms, that removes the possibility of confounding effects

from correlated traits. We apply 3D computer models of the diatom *S. niagarae* to simulated sinking experiments in a computational fluid dynamics software space. Simulations in 3D computer space allow us to create models of the diatom frustule with and without spines, and to vary cell size. Most importantly we can change a single trait on a computer model without affecting correlated traits. For *S. niagarae,* creating spines on the frustule adds 6-24% to the cost of the silica contained in the frustule (Mohan *et al.* 2021), hence we also aim to quantify one of the associated benefits, the change in sinking behavior, of spine construction.

Methods

We design a 3D computer simulation to examine differences in diatom sinking behavior with and without spines. We construct 3D computer models of the diatom *S. niagarae* and input the models into a computational fluid dynamics software. The software solves Navier-Stokes equations to produce robust estimates of fluid and diatom behavior. We can run simulations with spined and spineless models in tandem to measure the differences in sinking behavior. We choose this species for a first look into differences in sinking behavior induced by trait evolution because *S. niagarae* has the capacity to evolve rapidly and resides within a species complex whose major phenotypic difference is the ratio of spines (Theriot *et al.* 2006; Theriot & Stoermer 1984).

Following methods in Mohan, Saros, and Stone (2021), we construct 3D computer models of the diatom *S. niagarae*. 3D models of *S. niagarae* are created by taking measurements of the phenotypic traits that comprise the frustule (diatom shell). These measurements are averaged across the size range and used to construct 3D models. In this case we use Autodesk CAD software. First the base of the frustule (discoid) is constructed, then other traits are added to the discoid, *e.g.* spines, pores, girdle band. Then 3D models of *S. niagarae* are placed in a

computational fluid dynamics (CFD) software, in this case AutodeskCFD software. We set up a computer-simulated experiment designed to test the change in sinking behavior of two models: one in which *S. niagarae* has spines which reflects reality and is the control group, the other in which the spines are removed, represent a single trait modification, and is the experimental group. The modified experimental model has no other adjustments. The traits such as fultoportulae and rimoportulae (pores on the frustule), which are correlated in nature and would confound results, have been left unmodified. We do this so that the only trait difference from control to experimental group is a single trait, spines, which prevents confounding results from correlated trait influences.

The two diatom models (with and without spines) were placed in a simulated column of water and allowed to fall under the force of gravity for 2000 μm (Figure 3.1). We then repeated this experimental simulation with models across four cell sizes to account for diatom size diminution from 50 to 35μm (Figure 3.2). We cover this size range so that we can compare sinking behavior across a broad range of sizes and ensure results are transferable across the size of a population. Results are saved in the CFD software every 0.1 second throughout the simulation.

Computational fluid dynamics software does not typically operate at the microscale and thus our models were too small to use true to scale models. We employed the scaling law and principals of similitude to alter the densities of each model and water so they would interact true to reality when increased to the millimeter scale. Properties of size, density, and velocity cannot scale directly proportional to each other and must follow the scaling law to ensure proper modeled outputs. In simulation, length must be scaled from μm to cm to fit within software

capacity. To compensate for scaling we chose to scale these parameters to maintain time as a consistent variable from reality to simulation which maintains similitude across the results.

Reynolds number

$$R_e = \left(\frac{\rho V L}{\mu}\right) \qquad V_{model} = V_{reality} * \left(\frac{\rho_r}{\rho_m}\right) * \left(\frac{L_r}{L_m}\right) * \left(\frac{\mu_m}{\mu_r}\right)$$

Pressure coefficient

$$C_P = \left(\frac{2\Delta p}{\rho V^2}\right),\ F = \Delta p L^2 \qquad F_{reality} = F_{model} * \left(\frac{\rho_r}{\rho_m}\right) * \left(\frac{V_r}{V_m}\right)^2 * \left(\frac{L_r}{L_m}\right)^2$$

The diatoms were set to be comprised of silica glass. Diatoms are 10% to 70% amorphous silica (density ~ 2600 kg/m^3), the rest of the frustule being composed of proteins and sugars (density ~ 1300 kg m^3. Mass of a 35μm diameter with 2 valves is 680 μm^3 * 2600kg/m^3(.0026ng/m^3) + 9220 μm^3 * 1300 kg/m^3 (.0013ng/μm^3) = 13.754 ng or overall density of ~1,400 kg/m^3 (Mohan *et al.* 2021; Schmid *et al.* 1981)). Water parameters were scaled for density and viscosity in proportion to the size differences following scaling laws. Following these scaled parameters, we are able to retain mathematical similitude for gravity and time which are the critical outputs to compare across diatom size and trait differences.

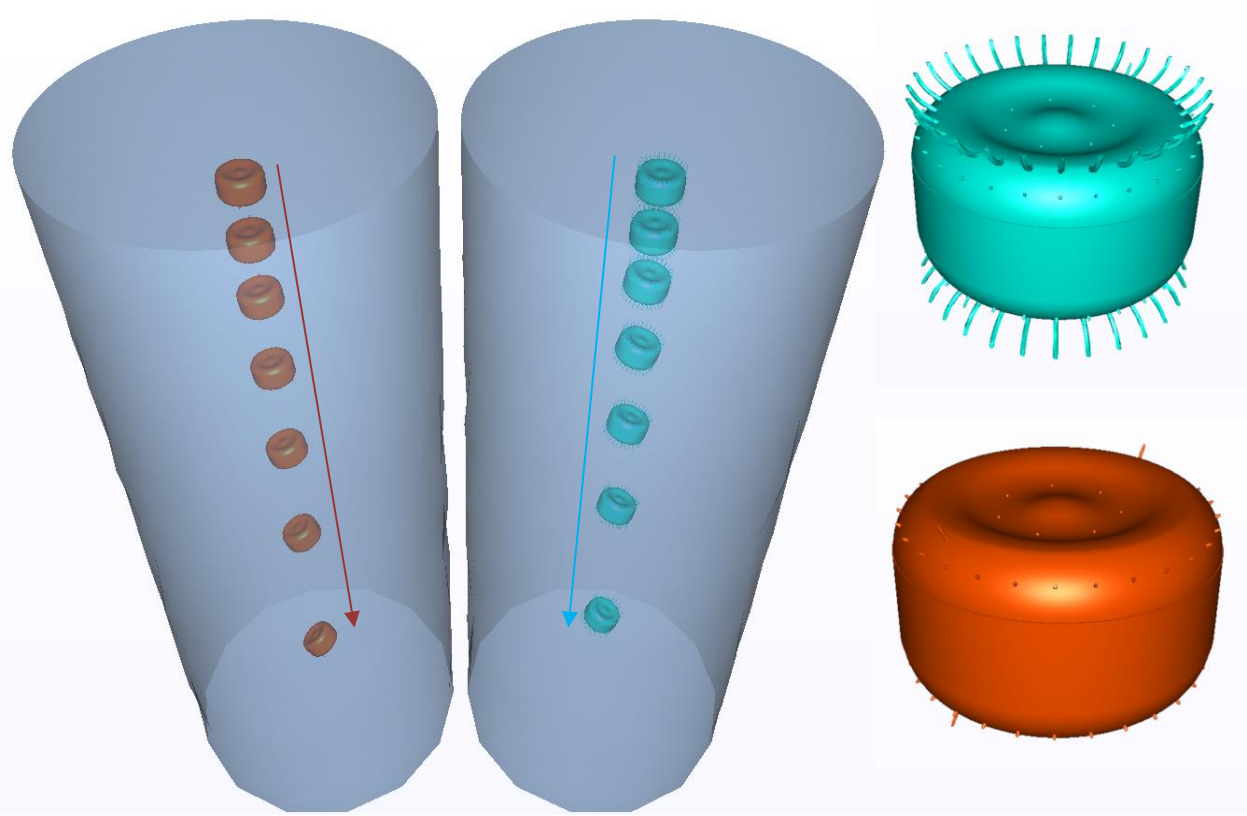

Figure 3.2 3D models of *S. niagarae* with spines (blue) and with the spines removed (orange). 3D models are simulated in columns of water (blue cylinders). These models were subject to gravity (arrows indicating gravity direction) under standard temperature and pressure. Results calculated in AutodeskCFD software. Each diatom model shown in the water column represents a time step interval of distance sunk over time. Large images of the diatom models shown on right exhibit the realistic model of *S. niagarae* (top, blue) and the experimental model where the spines have been removed (bottom, orange).

Diameter µm	Frustule volume (μm^3)	cytoplasm volume (μm^3)	Density ($kg/m^{3)}$
35	680	9260	1389
40	1042	13398	1394
45	1564	17521	1407
50	2232	23554	1413

Table 3.1 Input values for each model size class that combines the volume of amorphous silica glass with the volume of cytoplasm, chlorophyll, and other organic compounds in a diatom thus we assign the combined cell density to each simulation.

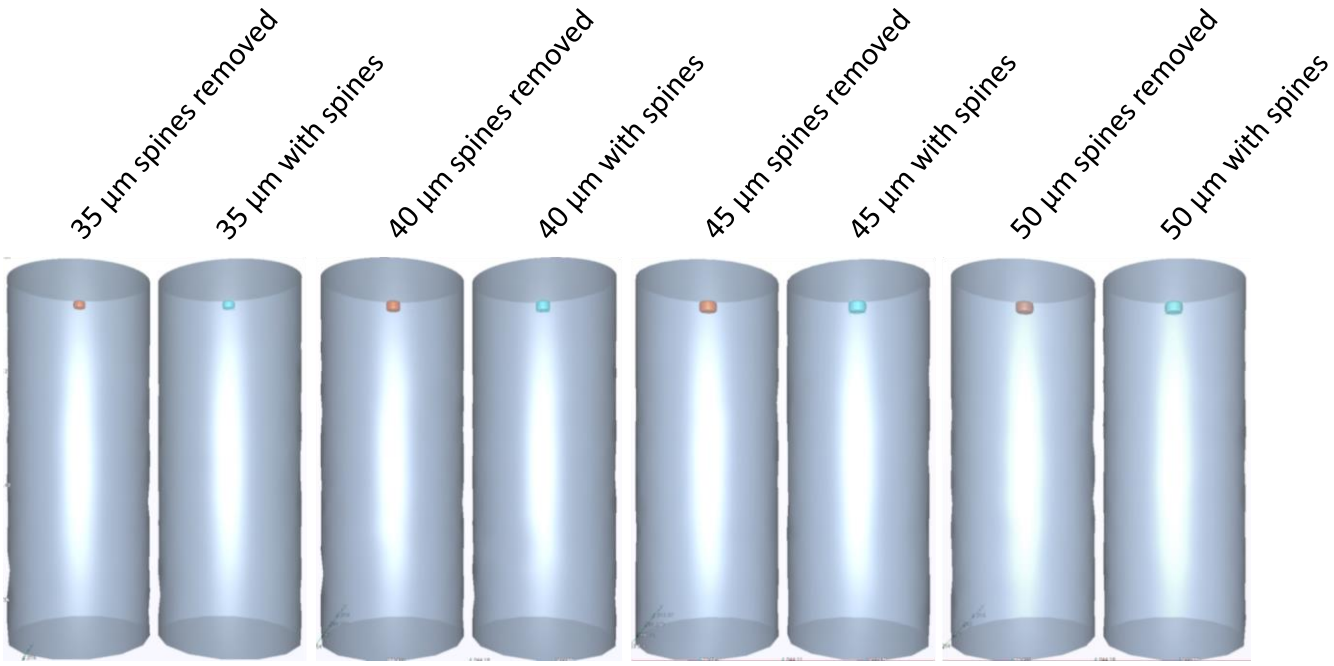

Figure 3.3 Experimental setup expanded from Fig. 3.1 of multiple water columns with parallel simulations of models with spines and spines removed sinking through their respective water columns. Four size classes of diatom models with diameters 35 µm, 40 µm, 45 µm, and 50 µm were simulated with a sinking distance of 2000 µm.

Results

Across all the model sizes, the diatoms that had the spines removed sank farther than the models with spines at each time slice. We present the model with a diameter of 50µm in Figure 3.3 to illustrate the results of one of the simulations in a 3D rendering of each time slice. We observe that diatom models without spines sink further than their spined counterparts (Figure 3.4). The difference in distance sunk kept increasing over time throughout the simulation, with the smallest diatom (35 µm) having the largest difference in sinking distance (234 µm difference at the end of the simulation) between control (with spines) and experimental (spines removed). The largest cell size (50 µm) had the least difference between control and experimental models,

having a difference of 168μm at the end of the simulation. These represent a 11.7% reduction in sinking for the 35 μm pair and 8.4% difference for the 50 μm pair (Table 3.2).

We also observe that sinking rate is reduced from larger to smaller diameter diatom models. In Figure 3.4 we see that the 35-μm model with spines took ~2.7 seconds to sink 2000 μm whereas the 40-μm diameter model with spines took ~2.5 seconds, the 45-μm diameter model took ~2.4 seconds, and the 50-μm diameter model with spines took ~2.3 seconds to sink past 2000 μm (Figure 3.4). This result is expressed across the size range of models in the distance traveled after 2.2 seconds. Over that time, the smallest (35 μm) spineless model sank 1439 μm, but with spines sank 1232 μm. The next size up (40 μm) sank 1628 μm (spines removed) and 1445 μm (with spines). The next largest models (45 μm) sank 1782 μm (spines removed) and 1588 μm (with spines), whereas the largest models (50 μm) sank 1852 μm (spines removed) and 1685 μm (with spines) (Table 3.2). Summarizing these data, we observe the experimental group models where spines have been removed accelerate faster and sink faster than the control group models with spines.

We also find that there is a variable cost to benefit of trait construction across the size range of these diatoms. For example, the cost of spine construction for the largest (50 μm) models in our simulated experiment represent 12% of the silica dioxide used in frustule construction, in turn the diatom sank 8.4% less in our simulation. Constructing the spines on the smallest (35 μm) model cost 24% of the silica dioxide in the frustule and result in 11.7% reduction in sinking in our simulation.

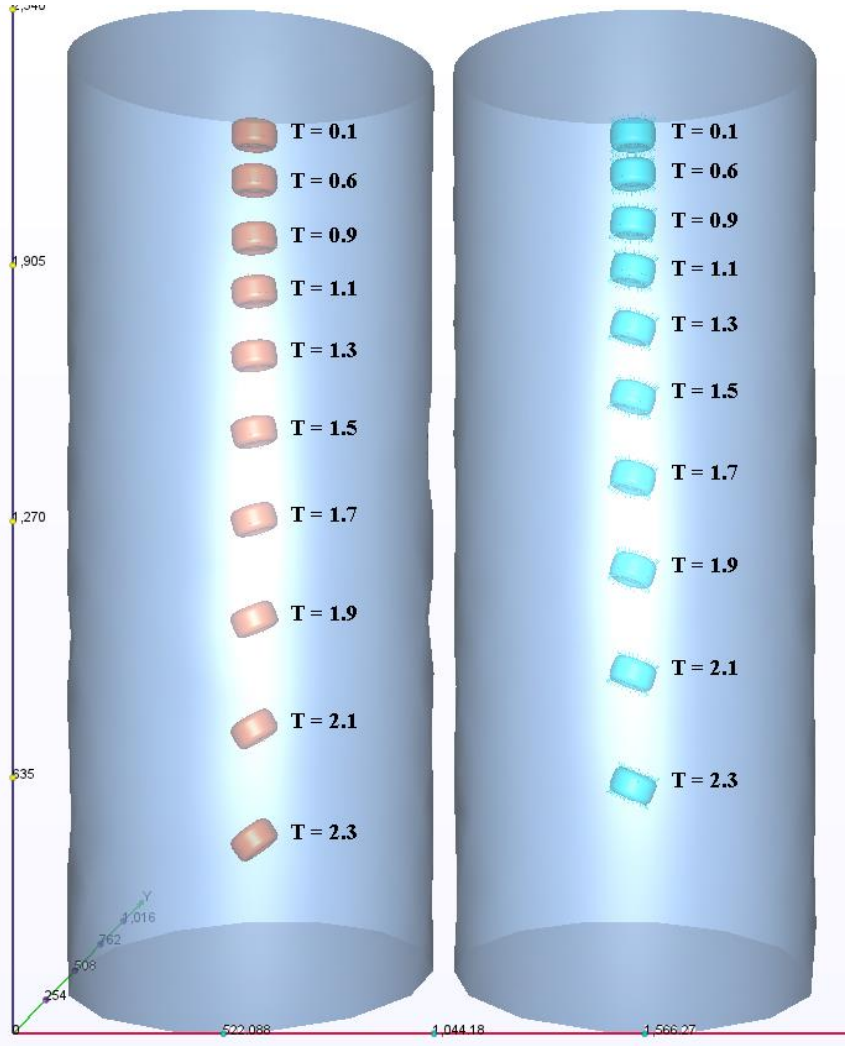

Figure 3.4 Distance traveled over time displayed as a representative rendering of the CFD software simulations. All models shown in blue are the control models that represent reality (with spines). All data represented in orange are the experimental group models (spines removed). The image rendering is created by overlaying the models in simulated water columns and saving images every few time steps. Overlapping positioned timesteps have been removed in the left side image for clarity. The image is of the results of the 50 μm diameter model. The visualization shows that at each time stamp, the orange model where spines are removed has sunk farther than the blue control model (with spines).

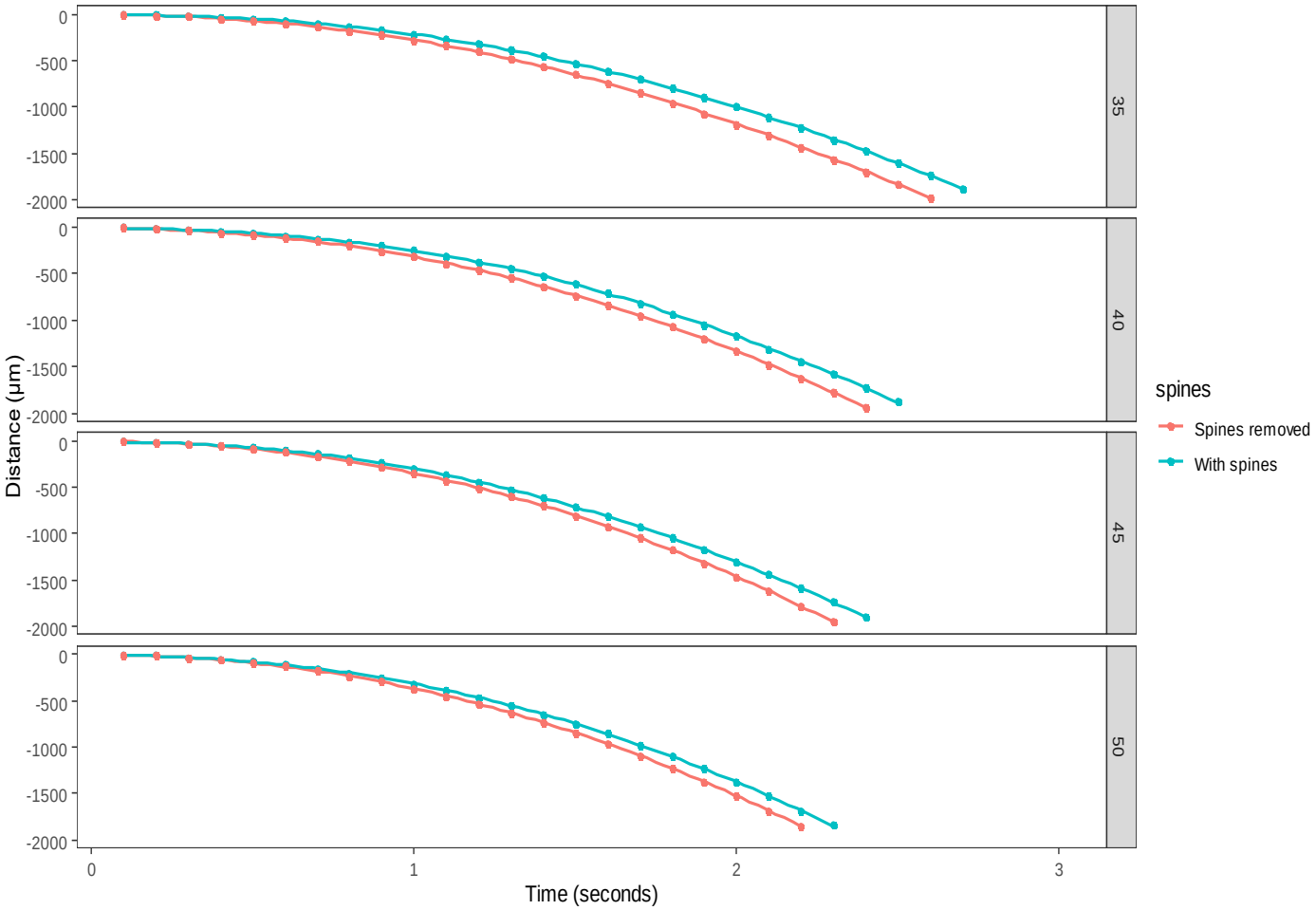

Figure 3.5 Distance sunk over time of each model. Panels are separated by model diameter. Models with spines (blue), being above the models that have had spines removed (orange) shows that for each simulation the model with spines took a longer time to sink the same distance i.e. models with spines sank slower. Comparing across models we see that the smaller diatom models took longer to sink than the larger diatoms.

Comparing the resource cost to benefit of constructing spines across the size range in these models (Figure 3.5), we observe the difference in sinking rate after 2.0 seconds of simulated sinking. We choose this time point for comparison because it is prior to significant tumbling action and before any of the models exceed the simulations boundaries. Differences in sinking at 2.0 seconds give an ~8 – 9% decrease in sinking distance (Figure 3.6). We observe that

constructing spines on the 35-µm model costs the least in terms of absolute silica resources and provided the greatest reduction in sinking. The largest model (50 µm) spends the most amount of silica constructing spines, however it receives the least sinking reduction benefit. The larger diatoms spent more in terms of raw silica than the smaller diatoms however as a percent of the total frustule, small diatoms spend ~24% and large diatoms spend ~6%.

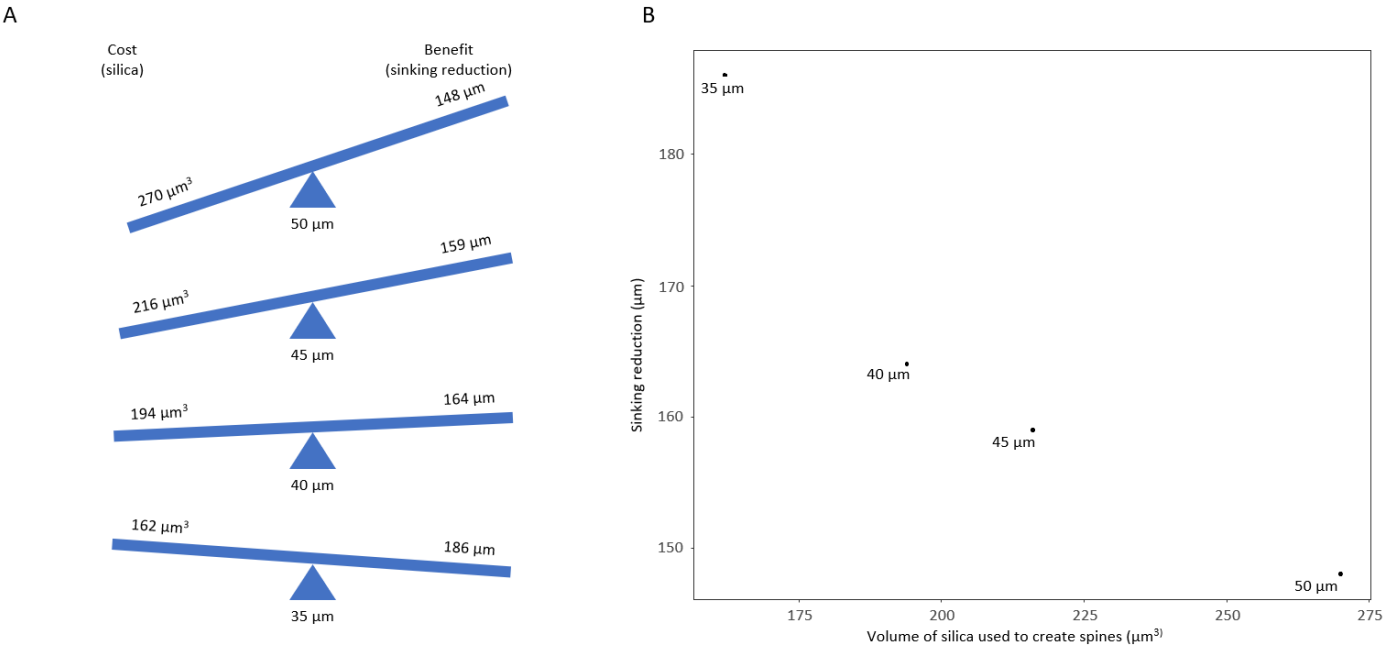

Figure 3.6 Cost versus benefit of spine construction on *S. niagarae*. Cost is the amount of silica required to construct spines for the size range (Mohan et al, 2021) and the benefit herein is the difference in sinking between models with spines and having removed the spines after 2 seconds of simulated sinking. Panel A exhibits a cost benefit balance framework to visualize the difference is silica cost to the difference in sinking. Panel B plots the experimental cost (volume of silica used to create spines) and the response (sinking reduction) across the model sizes.

Time	35 spines removed	35 with spines	difference	40 spines removed	40 with spines	difference	45 spines removed	45 with spines	difference	50 spines removed	50 with spines	difference
0.1	-5	-5	0	-5	-5	0	-5	-5	0	-5	-5	0
0.2	-17	-16	1	-18	-17	1	-18	-18	0	-18	-18	0
0.3	-32	-27	5	-35	-31	4	-37	-35	2	-38	-36	2
0.4	-49	-39	11	-56	-47	9	-60	-54	6	-63	-57	6
0.5	-73	-55	18	-81	-66	15	-90	-78	12	-94	-83	12
0.6	-102	-76	26	-114	-91	23	-126	-107	20	-133	-115	18
0.7	-139	-103	36	-154	-122	32	-170	-143	27	-179	-154	25
0.8	-181	-136	45	-201	-159	42	-222	-186	35	-234	-200	33
0.9	-230	-175	54	-255	-201	54	-281	-238	43	-297	-254	43
1.0	-283	-220	63	-317	-250	67	-348	-298	50	-368	-316	52
1.1	-342	-271	72	-385	-307	78	-424	-367	57	-448	-387	61
1.2	-409	-327	83	-461	-373	88	-508	-443	65	-535	-465	70
1.3	-483	-389	94	-543	-445	98	-599	-526	73	-630	-551	79
1.4	-565	-458	107	-633	-525	108	-698	-616	81	-733	-645	88
1.5	-652	-533	119	-731	-614	117	-805	-713	92	-844	-747	98
1.6	-747	-615	132	-836	-711	125	-920	-816	104	-965	-857	108
1.7	-849	-702	147	-949	-816	133	-1044	-927	117	-1094	-976	118
1.8	-958	-796	162	-1071	-929	142	-1176	-1046	130	-1231	-1102	129
1.9	-1071	-896	175	-1201	-1048	153	-1315	-1171	144	-1376	-1237	139
2.0	-1189	-1003	186	-1338	-1174	164	-1463	-1303	159	-1528	-1380	148
2.1	-1313	-1116	197	-1481	-1308	173	-1618	-1442	176	-1687	-1530	157
2.2	-1439	-1232	207	-1628	-1445	182	-1782	-1588	193	-1852	-1685	168
2.3	-1566	-1352	214	-1780	-1585	195	-1953	-1741	212		-1846	
2.4	-1698	-1477	221	-1936	-1728	208		-1899				
2.5	-1835	-1608	228		-1877							
2.6	-1977	-1743	234									
2.7		-1882										

Table 3.2 Linear displacement on the Z axis (downward) for each model over time. Run time for each model ended when the model exceeded -2000 displacement in the Z axis.

Discussion

We use engineering tools to quantify single trait function in a way that removes the influence of correlated traits on selection pressure. Using 3D models of microscopic organisms, we can manipulate test parameters in computer simulation to artificially modify an organism's

phenotype. In Mohan, Saros, and Stone (2021) we learned the resource cost of a single trait and herein we quantify one of the benefits of a single trait. We have revealed the effect of a single trait, *i.e.,* spine construction, on the selective pressure of sinking behavior. Exploiting the capabilities of modern engineering tools, specifically by combining 3D modeling software and the associated suite of analysis that can be performed in computer simulation, we can explore previously unattainable areas in the physiology, phenotypic evolution, and trait function of microscopic organisms.

These results are in accordance with predictions from Stokes' Law that the larger diatom cells will sink faster than the smaller cells, yielding a positive correlation between cell size and sinking rate (Waite *et al.* 1997). However, Stokes equations were developed to approximate the sinking behavior of spherical objects with very small Reynolds numbers (Batchelor 2000). Diatoms are not typically spherical, except when they undergo the auxosporulating phase of their sexual reproductive cycle, which is also when they are at their largest size and would require higher upward force to keep them from sinking. Small diatoms spend less silica than larger diatoms on spine construction and receive more of a benefit in reduced sinking. Figure 3.6 highlights the differences in sinking rates across our simulated experiment. With small diatoms spending ~24% of the frustule volume and large diatoms ~6% on spine construction, then spine construction may be a greater metabolic burden on small diatoms.

Diatoms exhibit different sinking rates in relation to the symmetry of spine arrangements. Padisak et al. (2003) used ~1-10 cm scale models made from a PVC based modeling material with a density of 1.84 g/cm^{-3} and sank them in glycerine so that the density ratio from model to liquid was ~1.50, admittedly slightly higher than the ratio from diatom to lake water but close. While the density ratio was considered in their experimental design, they scaled the viscosity by

a factor of ~15x. Solving the scaling law between these models would have required the models to sink into a liquid with much higher (~10,000x) viscosity rendering their conclusions not likely to be transferable. Because fluid dynamics software is scalable for every parameter, it is able to accurately scale the density and viscosity of the fluid medium giving us more accurate insights of the sinking behavior of diatoms.

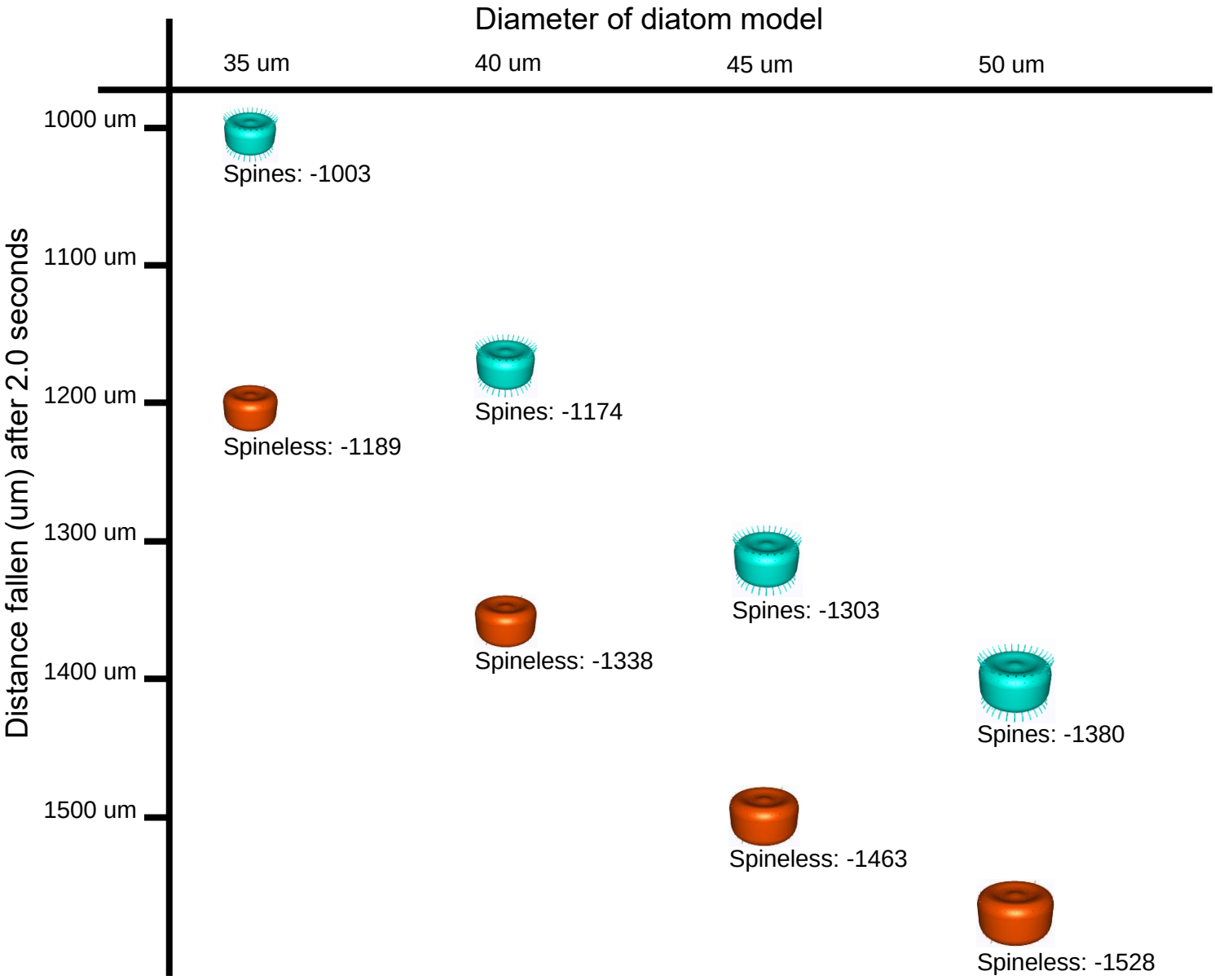

Figure 3.7: Graph highlighting the differences in sinking distance after 2.0 seconds of sinking for spines and spineless models. Data from Table 3.2.

S. niagarae usually persists during the summer stratification phase of North American temperate lakes that have high silica (Interlandi *et al.* 1999; Kilham *et al.* 1996). We find that spines reduce sinking of *S. niagarae*, thus playing an integral role in facilitating the success of the species during summer stratification. In Chapter 4, we find that hotter years result in small diameter *S. niagarae* population distribution, and herein we find that smaller diatoms within a population are more resistant to sinking. Much in the way different sized diatom species are used to infer past mixing depths (Saros *et al.* 2012; Saros & Anderson 2015), we find that size change within a species may suggest changes in lake mixing and thermal structure.

Further applications of 3D modeling

3D simulations can be used to test trait function. We suggest that further applications of these methods can elucidate function of phenotypes of extinct species. One of the great mysteries that may be directly tied to the spine functions revealed in this study is the replacement of the genera *Actinocyclus* and *Mesodicton* by *Stephanodiscus.* This replacement occurs in North American lake deposits during the Late Miocene (Krebs, Bradbury, and Theriot 1987; Theriot and Bradbury 1987). A notable difference between these genera are that *Actinocylcus* and *Mesodictyon* do not exhibit spines while some large *Stephanodiscus* do exhibit spines. We suggest using 3D simulations to reveal selective forces on fossil species may elucidate reasons for extinction.

S. niagarae has rapidly evolved into new species; most notable is the shift in spine distribution across the *S. niagarae* species complex which is only circumstantial evidence for selection pressures correlated with spine morphological changes (Theriot *et al.* 2006). Expanding our 3D simulation methods to analyze the resource cost to trait functional changes across evolving species complexes is likely to reveal important drivers in phenotypic evolution.

There are numerous parameters to explore when placing 3D diatom models in computational fluid dynamics space. Most of the problems with these methods involve deciding where to draw the limits of a particular study. Differential morphology within and across taxa present multiple lines of further research. Exploring environmental gradients is likely a promising field of exploration we omitted in this study. The viscosity and density of water changes greatly with temperature and microscopic life responds to changes in fluid properties to a greater degree than macroscopic organism (Guasto *et al.* 2012; Purcell 1977). The sinking rate kept increasing over the entire simulation which indicates that these models did not reach their terminal velocity. We were also not able to render the largest sizes of *S. niagarae* into this software because of the limits of computational power available for this study. There are also a host of other possible software methods to use such as particle-based simulations vs. 3D mesh-based software. All the above examples address the same issue: technology and computations could continue to be improved perpetually but eventually researchers must decide when to trade improving complexity, accuracy, and transferability for viable comparative results. Since all models are wrong, the scientist should follow Occam to seek simple descriptions of natural phenomena rather than overparameterize *ad nauseam* (Box 1976).

Ecological context

Sinking is an integral part of diatom ecology. Smetacek (1985) proposed that sinking is a crucial part of bloom survival strategy for planktonic diatoms. We show herein that larger *S. niagarae* sink faster than smaller ones and suggest that variable sinking rate across the size range of a plankton species diversifies the hydrodynamic conditions that the species can persist in or sink out of. Sinking and buoyancy can also be regulated in some plankton diatom species, upon nutrient depletion in the water, sinking can increase. Sinking rates can decrease upon

encountering nutrient rich water layers indicating that buoyancy can be physiologically controlled (Bienfang *et al.* 1982; Smayda 1970). If buoyancy and sinking is controlled physiologically, then we should point out that the spined models resisted change in velocity to a greater degree than the models where spines had been removed. These results in this perspective suggest that spines may act as a stabilizing structure to reduce the impact of external force and increase the effective inertia of the diatom.

Predation and spines

Speculation that spines are defensive structures persist, however observations of grazing give mixed interpretations. Capriulo & Carpenter (1980) found that small zooplankton did not feed upon spined diatoms even while consuming a large portion of the standing Chl *a*. So while spines are an effective defense against small grazers, spines increased the probability of consumption of diatoms by copepods because the spines increased the likelihood of detection by larger zooplankton (Gifford *et al.* 1981). Consumption by specialist zooplankton may be advantageous given that some species of diatom are able to survive gut passage through copepods and that sinking and overwintering are an integral part of diatom lifecycle (Kruse *et al.* 2009; Lurling 2021; Pancic´ *et al.* 2019). Lurling (2021) also found that effective defense against generalist grazers *e.g. Daphnia* and *Bosmina* is restricted to toxicity and colony formation. Preferential grazing away from spined diatoms has been observed in taxa with extremely large spines such as *Thalassiosira* and *Cheatoceros* (Gifford *et al.* 1981). Spines also influence the tumbling and spin of a cell under shear flow which we did not explore in this study (Nguyen *et al.* 2011).

Conclusions

We offer a solution for testing phenotypic influences on natural selection that precludes the convoluting influence of correlated traits. We find that spine construction creates resistance to acceleration and sinking rate. The ability to resist external forces on the hydrodynamic properties of a microscopic organism increases the influence that other, possibly internal, forces to define the organism's behavior in the water column.

CHAPTER 4 ASSESSING THE CLIMATE, WEATHER, AND NUTRIENT INTERACTIONS ON SILICA BURIAL AND SIZE STRUCTURE OF DIATOM POPULATIONS

Introduction

Organisms exchange matter and create complex flow paths across ecosystems. These flow paths vary in mode, strength, timing, and direction (Cohen *et al.* 2016). Quantifying flow path connectivity is critical in developing ecosystem functional models that explain past trends, predict future changes, and unite ecology with hydrology (Tetzlaff *et al.* 2007). Carbon and nitrogen biogeochemical cycles are strongly intertwined with the silica cycle, which is well associated with primary productivity in aquatic systems. However, the scale, pattern, and controls of the global silica pool are poorly constrained (Harrison *et al.* 2012). The realization that silica is strongly intertwined with other nutrients and primary productivity has resulted in calls for reassessment of the global silica cycle (Treguer & De La Rocha 2013). Reassessing silica has revealed that biogenic silica from diatoms constitutes significant global sinks for other nutrients such as aluminum (Liu *et al.* 2019).

Silica flow paths can be traced from the lithosphere, across ecosystems, through time, and may have been altered by diatom species radiations (Rocha 2002). Until recently we lacked the ability to quantify the amount of silica that an individual diatom contained. Mohan et al. (2021) developed a three-dimensional computer modeling method to estimate the volume of silica contained in individual diatom cells. Scaling this three-dimensional approach to quantify population-level silica cycling is the next challenge. We do not know how much silica a population of diatoms uses across the spectra of size and abundances. Without this knowledge we are unable to quantify how diatom community turnover will influence silica cycles and affect

ecosystem functions. As ecosystems change under global climate and anthropogenic influence, we need to be able to predict how diatom community turnover will affect matter and energy flow paths to be better prepared to protect aquatic ecosystem services under global change.

Kilham (1971) introduced a unifying hypothesis for planktonic diatoms in lacustrine systems, that when all other nutrients are not limited, silica concentrations strongly influence species abundances. Thus, only in eutrophic lakes will silica be a driver of species composition. This hypothesis arose from earlier work that suspected silica concentration played a role in shaping seasonal succession of phytoplankton where species with low nutrient requirements are not dominant until the species with higher nutrient requirements have bloomed and reduced nutrient concentrations (Hutchinson 1967). Silica concentrations in the water column are known to become depleted in response to increased diatom production. When phosphorus concentrations are enriched, diatom productivity increases which leads to depletion of silica (Schelske et al. 1986). Our aim is to quantify the flow path of silica at the population level, specifically to quantify the annual amount of silica buried in lake sediments by diatom populations. We also assess the ecological drivers that change the amount of silica that a population of diatoms use each year. Finally, we use these data to address if this new metric is useful as a proxy for paleontological reconstructions.

To accomplish these objectives, we utilize an annually resolved (varved) lake sediment archive. Annual resolution allows us to explore whether sedimentary nutrients, weather and climate, or conditions of previous years (*i.e.* lag effects) play a role in determining the amount of silica buried by a diatom population. We first quantify the amount of silica that a single species buried each year by measuring the size structure of each year's population. We then factor in the silica volume for each cell size of this diatom's population and multiply by the abundance. When

summed across all size classes, this provides total silica buried by a population of diatom, a novel metric in diatom paleoecology. We conducted exploratory statistics to identify potential drivers of total silica buried by a population and how it might interact with other nutrient flow paths.

Methods

Site description

We extract the data presented herein from the sedimentary archive recovered from Herd Lake, Idaho, USA (44.089321°, -114.173895°). The archive from Herd Lake was selected for this study because of the remarkably thick (~1 cm), continuous varve couplets (annual layers) as well as the low diatom species diversity in this system. We analyze a core taken in 2011 that contains continuously varved sediment back to 1927 (Shapley *et al.* 2019). These varves were thick enough that we were able to subsample sediments from individual years. Most sedimentary archives are not able to parse out individual years and are thus subject to time averaging, meaning one cannot assess diatom populations each year. This annual aspect to our data also allows us to assess the influence that each previous year's silica burial (i.e. silica removal from the water column) may have had upon the diatom population and community in subsequent years. The low diatom species diversity simplified our methods for quantifying the silica content of a population for a single species because we were able to parse out species on an automated rapid measuring system (FlowCAM cytometer).

Silica buried by diatom populations

Diatom populations and community structure were revealed by processing each yearly subsample according to standard methods (Battarbee *et al.* 2001). The resulting diatom residues were placed on microscope coverslips, dried, and mounted on slides in Naphrax, a highly

refractive mounting medium. Absolute abundances were determined by counting diatom valves and comparing to abundance of a known concentrated spike of 14um plastic microspheres added to each subsample. Diatom species abundances were enumerated at 1000x magnification under an Olympus BX51 light microscope. Diatom enumerations revealed the community structure and absolute abundance of each population. Further analysis was required to measure the size dynamics of each population.

We implemented a Fluid Imaging Technologies (FlowCAM) cytometer to quantify the size structure of diatom populations. The FlowCAM consists of a flow cell which directs fluid through a small aperture, and a laser particle detector which controls the imaging system to rapidly image microscopic particles suspended in fluid. Implementing a FlowCAM cytometer allowed for rapid identification and measurement of individuals in the population of *Stephanodiscus niagarae* for each subsample, which constituted up to 33% of the diatom community. The FlowCAM can be used to automate diatom size measurements (Spaulding et al. 2012; Bishop and Spaulding 2017) by rapidly identifying particles passing by a microscope, imaging them, and measuring their shape. Individuals of *S. niagarae* were parsed out from other particles via a sorting algorithm based on the size range and aspect ratio of each particle. In this case we used 200x magnification in a 50-µm flow cell to pump samples at 0.1 ml per minute for 20 minutes to produce ~ 5,000-10,000 unique particle images per sample yielding ~ 500,000 particle images for the sample set herein. Visual confirmation of the sorting algorithm ensured a high degree of accuracy in identifying *S. niagarae*. Measuring the diameters of many *S. niagarae* allowed us to apply the silica volume formula developed for this species across the size range for each varved sediment year (Mohan et al. 2021). The techniques, analyses, and computations (Figure 4.1) were conducted via R programming language with the aid of the R packages

ggplot2, scales, dplyr, and ggridges (Wickham 2016; R Core Team 2020; Wickham and Seidel 2020; Wickham et al. 2020; Wilke 2021).

Variable selection

Variables for exploratory statistical correlations were selected based on ecological drivers that *S. niagarae* has strong association with. Variables were also selected to asses known regional effects on hydrological cycles to asses if *S. niagarae* responds to climate oscillations such as Pacific Decadal Oscillation (PDO) as in the case of plankton species in the northwestern United States (Stone *et al.* 2016). The varves in the Herd Lake sediment archive make it possible to assess possible influence of El Nino Southern Oscillation (ENSO) on *S. niagarae* and is included. *S. niagarae* is a drought indicator in this region (Interlandi *et al.* 2001, 2003). The Palmer Drought Severity Index (PDSI) is included in these variables to assess drought response in this core as well as various reanalysis data that parse out the annual, seasonal, and monthly temperature and precipitation parameters. Geochemical nutrient data (N, TP, OP, OxP, C) from analysis of this sediment core were procured to assess if the diatom populations and Si volumes of the population were associated or independent of other nutrient cycles in Herd Lake. We also assess the influence of possible competition or niche partitioning from the other major diatom taxon (*S. parvus*) in the sediment archive.

Assessing ecological drivers of diatom populations

To illustrate the utility of determining how much silica a diatom population buries, we compare the silica metric with a suite of data including diatom abundance, sedimentary nutrients, historical weather records, and the ENSO index. Diatom species abundance, population size structure, silica buried by a population, and geochemical nutrient data are determined from yearly subsamples from the Herd Lake sedimentary archive, while weather and climate data are

compiled from multiple sources and modeling to span from 1927-2011. We implemented a structural equation model to reveal the nuanced interactions among these measured and compiled data.

Weather and climate data were synthesized from a combination of historical temperature and precipitation records. Reanalysis and climate modeling data were used to fill in gaps where historical records proved patchy. We used these data to contribute to a structural equation model to reveal nuanced influences that weather and climate have upon nutrients and diatom community. Atmospheric data were retrieved from the National Oceanic and Atmospheric Administration's Working Group on Surface Pressure Niño 3.4 sea surface index. This index calculates the average sea surface temperature for the Niño 3.4 region defined by 5S-5N latitude and 170-120W longitude. Niño 3.4 data is expressed herein as the sea surface average annual anomaly (Smith 2018). Temperature and precipitation data were compiled from point data at the Herd Lake site using the ECMWF European Reanalysis of the 20th Century (ERA-20C) retreived from Climate Reanalyzer (https://ClimateReanalyzer.org), Climate Change Institute, University of Maine, USA. We investigated the influence that El Niño may play upon the diatom record in Herd Lake because nutrient pools are influenced by precipitation and there is a regional pattern of winter precipitation and spring water levels that is associated with sea surface temperature in the Pacific and El Niño oscillation (Harshburger *et al.* 2002).

Nutrient data were compiled via geochemical analysis in Indiana State University's Paleolimnology Laboratory and Geochemistry Laboratory. After subsamples for nutrients are dried and powdered approximately 0.1 g of sediment is into new 15 mL polyethylene centrifuge tubes. The sequential extraction method developed by Ruttenberg (1992) with modifications by Anderson & Delaney (2000) was used. The extraction includes four steps which isolate different

sedimentary associations of phosphorus: oxide-associated (OxP), authigenic, detrital, and organic-associated (OP). OxP is P that is loosely bound to Fe and Mn oxides and oxyhydroxides. OxP is typically formed when organic P is released into sediment pore water during decomposition and is bound to metals in sediment rather than being diffused into the lake water. NIST SRM1646a (estuarine sediment) was analyzed to evaluate methodical and analytical accuracy. All samples were analyzed using a Shimadzu UV-Visible scanning spectrophotometer at 880 nm using the molybdate blue color development technique (Strickland & Parsons 1972). Step 1 must be prepared for spectrophotometer analysis differently from Steps 2, 3, and 4. The CDB reagents (step 1) interfere with color development requiring an additional processing step that requires combustion and additional extraction with HCl prior to analysis. These data were analyzed from the Herd Lake sedimentary archive from 1927 which defined the temporal range of this study. This temporal range provides adequate overlap with historical weather and climate records to address the probable drivers of each variable with great confidence.

We used a path analysis to quantify the probability and magnitude of causal relationships among variables. Path analysis, in this case a structural equation modeling (SEM), is a causal modeling approach that allows us to explore the correlations within a network of variables and possible drivers. We apply this approach because the goals of SEM are to understand the correlation patterns among variables. SEM allows us to quantify multi-layer putatively causal networks of interactions among variables while accounting for covariates and covariances among variables. The goals and considerations of SEM align with our goals of assessing the interacting network of climate, weather, and nutrient variables which are generally considered to be causal drivers of diatom community composition and population dynamics (Julius & Theriot 2010). Three variables that were input did not return any significant interactions and are removed from figures for clarity. The previous year's *S. niagarae* silica mass, fall temperature (September –

November), and spring precipitation did not return any interactions, all other input variables for the SEM analysis are presented in the following figures. These analyses were conducted using the Lavaan package in R programming language (R Core Team 2020; Rossel 2012).

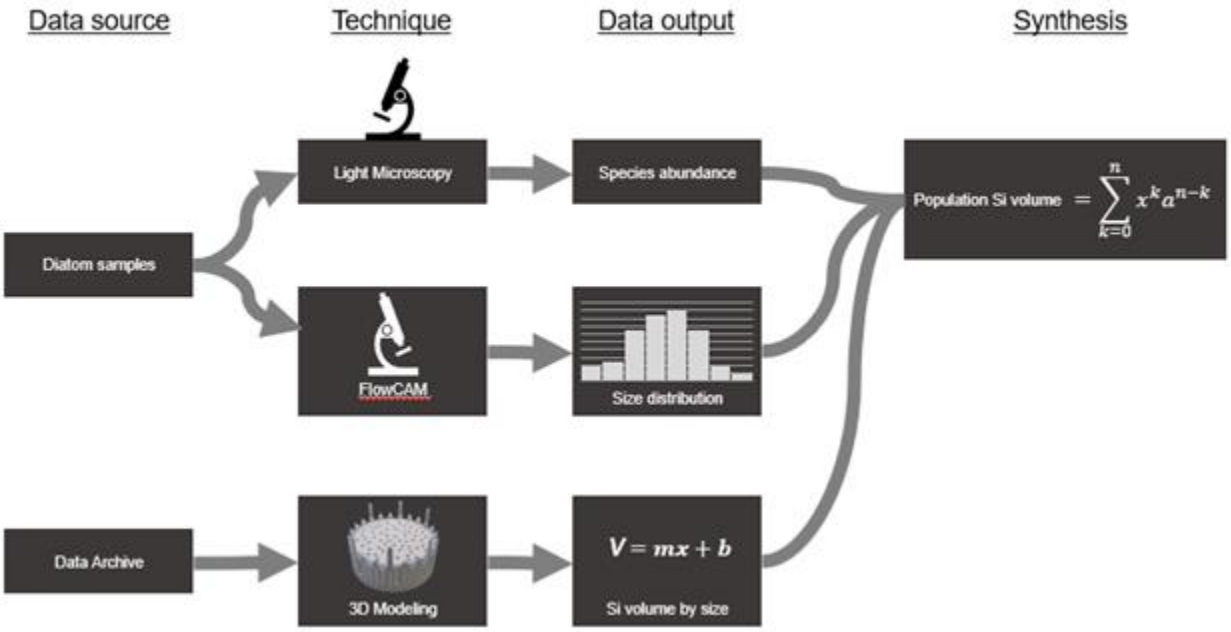

Figure 4.1 Conceptual flow chart of the data sources, analysis techniques, data outputs and synthesis used to estimate the total amount of Si that a population of diatoms is comprised of.

Results

Environmental data reveal some variability over the time span captured by the Herd Lake sediment record. Temperature in the region was warmer during the early parts of this record from 1927 through around the middle of the century (1950). From ~1950 temperature stayed cooler until ~1980. Warming temperatures have persisted since the early 1980s. This trend is observed across multiple monthly timeframes throughout our study time. The biggest departure from this trend is that during cold months (November – March) the mid-century cool phase of the record starts earlier ~1936 and lasts until ~1990 (Figure 4.2). Sedimentary nutrient concentrations exhibit low variability and lower than average values for the early and middle part of this record.

All of the nutrient values start to increase in the early 1980s and continue to rise through the end of this sedimentary record during 2011 (Figure 4.2).

In the Herd Lake record, diatom abundances increased after 1960. *S. parvus* abundances remained higher until the mid-1990s whereas *S. niagarae* decreased starting in the late-1980s. The size structure of *S. niagarae* appeared roughly inverse of its abundance during the middle of the century, meaning cells were smaller when they were more abundant. The mass of silica buried by each population of *S. niagarae* is higher from the mid-1960s through the mid-1980s, when there were more but smaller individuals (Figure 4.2).

We find a consistent yet subtle influence from El Niño upon the regional weather patterns. Positive El-Niño 3.4 index is strongly associated with slight decrease in summer temperature around Herd Lake, a slight increase in temperature during the spring (especially May), and increased precipitation during the summer. While the effect size is subtle for this influence it is consistent (Table 4.1, & Figure 4.3). During years with warmer months of May, organic phosphorus (OP) is reduced. OP is also reduced in years following increased size range in *S. niagarae.* OP is greatly increased during warmer summers. Nitrogen (N) is also greatly increased during warmer summers (Table 4.1, & Figure 4.3).

Throughout the sediment archive we find that the abundance of *S. niagarae* increases with OxP, OP, and higher summer precipitation. Drivers that reduce the abundance of *S. niagarae* are increased carbon (C), N, and total phosphorus (TP). The cell sizes in *S. niagarae* populations increase during warmer years, following previous years with high *S. parvus* abundance, and in years with increased N. We also find that the size of *S. niagarae* is reduced in years with higher OxP, when the previous year had larger sized *S. niagarae*, warmer springs,

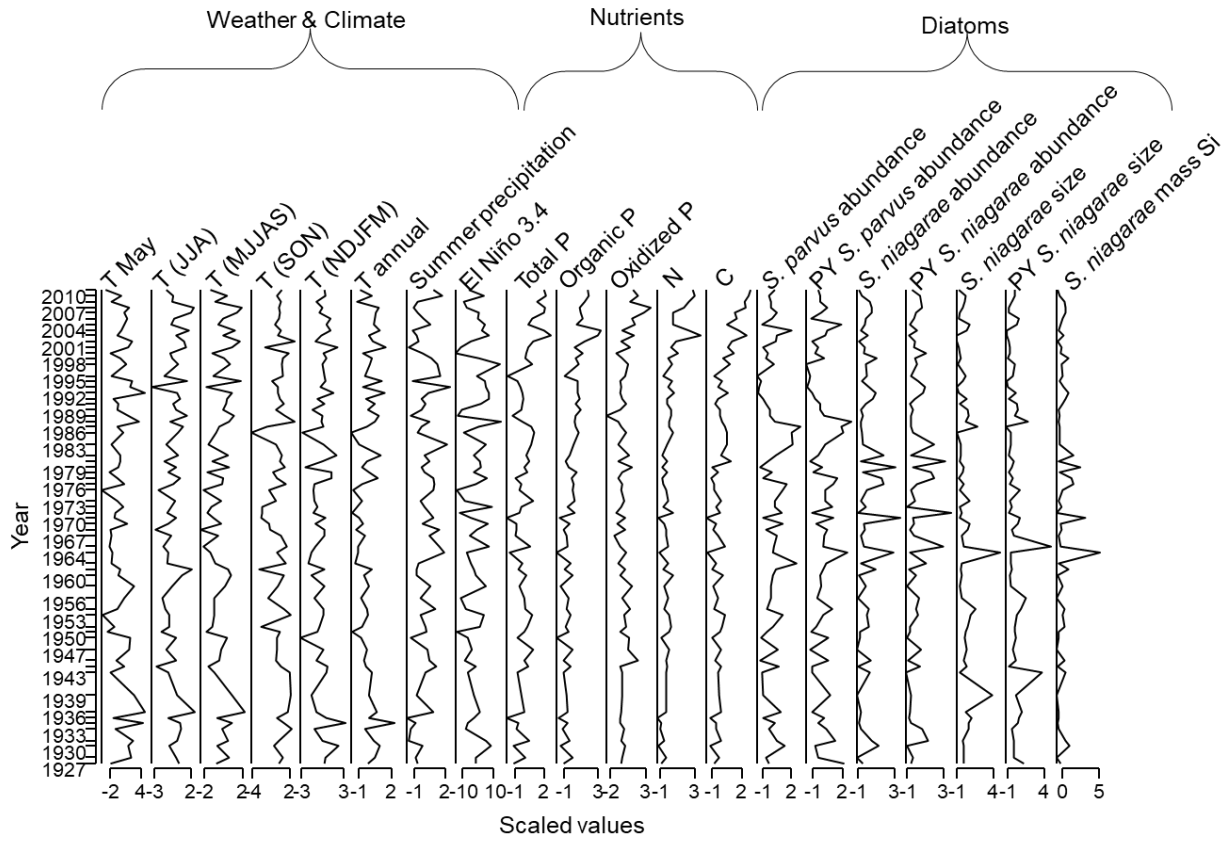

Figure 4.2 Stratigraphic plot of significant interactions of weather, climate, nutrient, and diatom variables as they are expressed over time from the Herd Lake stratigraphic record. Y axis represents time as calendar years in the common era, x axis values are expressed as scaled values relative to each variable. PY leading a variable indicates the previous year's value and is included to assess a time delayed response for some variables.

increased OP, and warmer winters. We observe that the total amount of silica in a population of *S. niagarae* increases with increased summer precipitation, increased OxP, and when the previous year had a higher abundance of *S. parvus*. Total silica in a population of *S. niagarae* decreases when TP is raised (Table 4.1, & Figure 4.3). We also find that the abundance of the diatom *S. parvus* increases with TP and when the previous year had high abundance of *S.*

parvus, *i.e.* increased *S. parvus* leads to increased *S. parvus*. The abundance of *S. parvus* decreases with higher N and OxP (Table 4.1, & Figure 4.3).

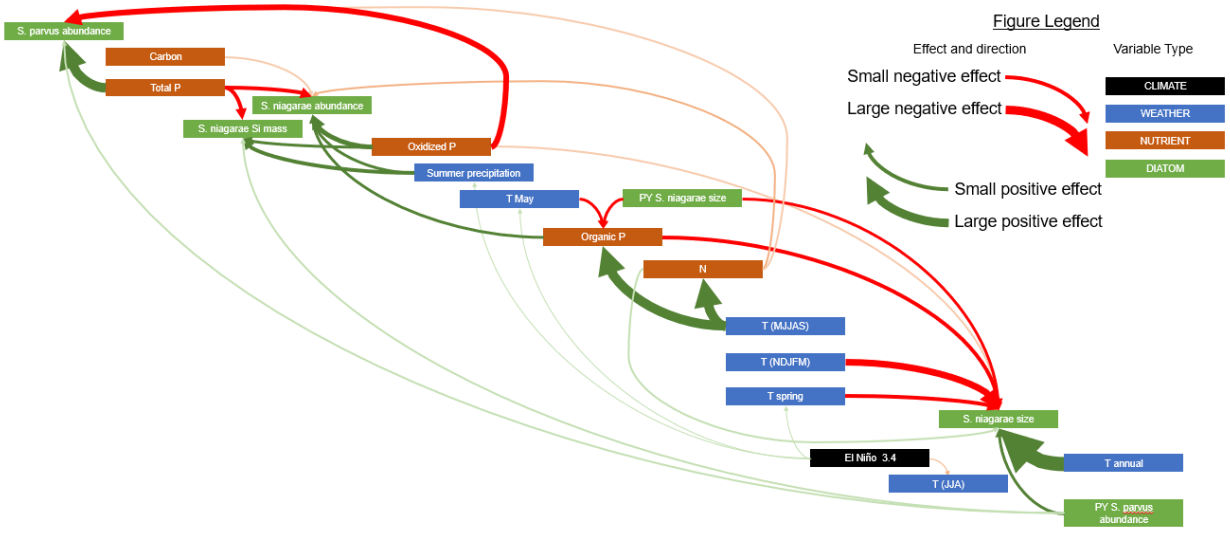

Figure 4.3 Major interactions of weather, nutrients, and diatom responses from a structural equation model using the Lavaan package in R.

Variable	Driver	Effect size	P value
T May	El Niño 3.4	0.06	0.026
Summer precipitation	El Niño 3.4	0.05	0.001
T spring	El Niño 3.4	0.05	0.015
T (JJA)	El Niño 3.4	-0.03	0.023
S. niagarae size	T annual	1.76	0.001
S. niagarae size	Previous year S. parvus abundance	0.35	0.000
S. niagarae size	Nitrogen	0.24	0.021
S. niagarae size	Oxidized P	-0.25	0.019
S. niagarae size	Previous year S. niagarae size	-0.36	0.008
S. niagarae size	T spring	-0.40	0.009
S. niagarae size	Organic P	-0.48	0.000
S. niagarae size	T (NDJFM)	-0.79	0.001
S. niagarae abundance	Oxidized P	0.52	0.000
S. niagarae abundance	Organic P	0.38	0.001
S. niagarae abundance	Summer precipitation	0.35	0.006
S. niagarae abundance	Carbon	-0.22	0.038
S. niagarae abundance	Nitrogen	-0.27	0.008
S. niagarae abundance	Total P	-0.46	0.000
S. parvus abundance	Total P	1.14	0.000
S. parvus abundance	Previous year S. parvus abundance	0.20	0.025
S. parvus abundance	Nitrogen	-0.24	0.013
S. parvus abundance	Oxidized P	-0.64	0.000
S. niagarae Si mass	Summer precipitation	0.44	0.001
S. niagarae Si mass	Oxidized P	0.38	0.000
S. niagarae Si mass	Previous year S. parvus abundance	0.21	0.027
S. niagarae Si mass	Total P	-0.43	0.000
Organic P	T (MJJAS)	1.17	0.006
Nitrogen	T (MJJAS)	1.11	0.015
Organic P	Previous year S. niagarae size	-0.32	0.022
Organic P	T May	-0.33	0.024

Table 4.1 Variables, drivers, and effect size (standard deviations) of significant ($P < 0.05$) interactions measured in the Herd Lake sediment archive.

Discussion

Quantifying Si flow paths

By modeling the Si burial capacity at the population and individual level, we can start to understand how diatom community shifts may affect local silica cycling and ultimately global Si models. Much of the global Si cycle consists of weathering from bedrock and transport across continents downstream to marine environments (Demaster 1981; Tréguer *et al.* 1995). The supply of Si to the world's oceans, however, does not follow a steady-state of export. Si export is modulated at least in part by accumulation of Si in lakes as biomass of primary producers (Frings *et al.* 2014). We have quantified part of the Si flow path to the individual and population level which is significant because the Si sink in lakes can represent a substantial fraction of imported Si (Hofmann *et al.* 2002). The deficit of Si mobilization from weathering to Si exported to the ocean is estimated from 21-27% (Frings *et al.* 2014). Changes in lacustrine diatom communities may lead to shifts in the global Si cycle. Herd Lake is positioned at the headwaters of the Salmon River which drains into the Columbia River and eventually into the Pacific Ocean. The Columbia River contributes considerable amounts of silicate, and nitrate into the Pacific Ocean. The nutrient-rich plume from the Columbia River primarily influences the timing of primary productivity peaks in the ocean near the mouth of the Columbia River which may influence fish production in the region (Anderson 1964). Herein we provide insight over the climatological controls at the headwaters that influence silicate plume size in the ocean. Specifically, we quantified the amount of Si buried by *S. niagarae* in Herd Lake every year since 1927. This Si would have otherwise been available to downstream communities. Unearthing the Si in upstream systems, quantifying the nutrient modulation, and revealing the controls that determine downstream nutrient availability informs global nutrient cycles and makes for more predictable nutrient cycling under future climate scenarios.

Ecological drivers

Using those data, we find that while there are similar drivers of Si mass to the abundance of *S. niagarae*, the drivers of size of *S. niagarae* are detached from the abundance and Si mass. We find that the major controls that increase the mass of Si buried by *S. niagarae* are summer precipitation which is enhanced by oxidized phosphorus and in years following more abundant *S. parvus*. The mechanisms linking mass of Si buried by *S. niagarae* to the controlling variables are elusive. Given that this is a newly created metric there are no mechanistic studies to reveal strong links in these processes. We can speculate that increased summer precipitation increases available Si via weathering and erosion into the watershed from soil and rock. The major driver that reduced the mass of Si buried by *S. niagarae* is total phosphorus (Figure 4.4). Mechanisms that increase Si burial along with OxP while decreasing Si burial with more TP could be regulated by micronutrient, Mn or Al, availability which end up bound to P after leaching from buried diatom cells, although we do not have direct evidence to support this mechanism. Because more Si is buried by *S. niagarae* during summers with higher precipitation, Si buried by *S. niagarae* may serve as a proxy to identify wetter summer conditions. The amount of Si buried by *S. niagarae* is also increased by elevated oxidized phosphorus levels but reduced when total phosphorus is elevated which suggests that this metric may be used as a proxy for phosphorous levels. We observe that the amount of Si buried by *S. niagarae* is not influenced by either the abundance or size range of *S. niagarae* which affirms this metric as independent from physiological characteristics and internal drivers. *Stephanodiscus* tends to thrive in silica-limited environments; this trend is pronounced in environments with very low Si to P ratio (Kilham 1971; Tilman et al. 1982).

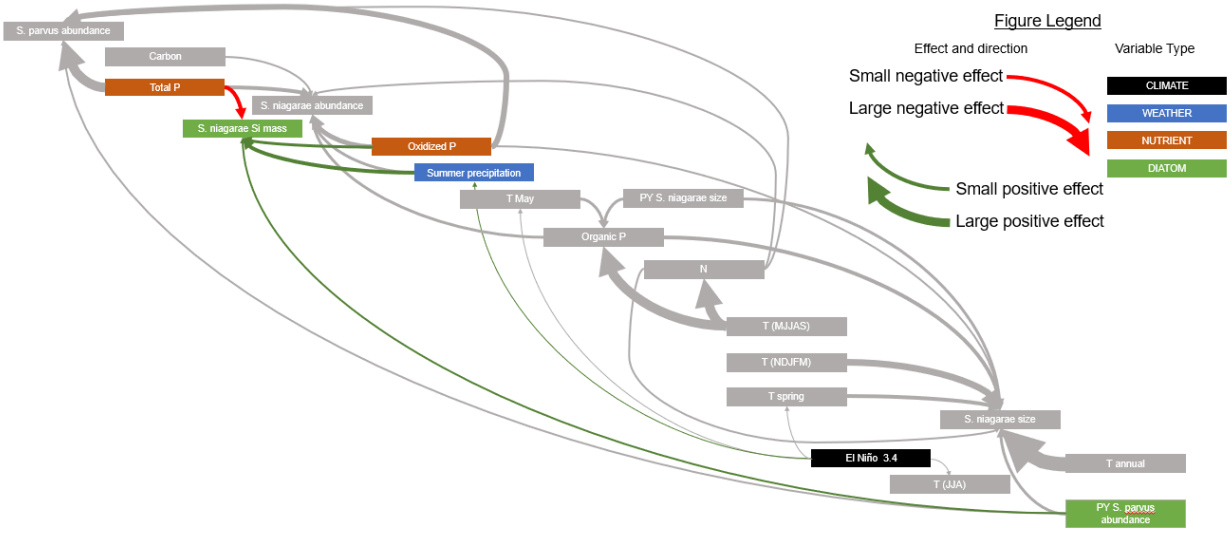

Figure 4.4 Results from the structural equation model highlighting the variables that exert pressures on the volume of Si contained in a population of *S. niagarae*.

Proxy assessment

Previously we quantified the amount of silica that is contained within an individual diatom (Mohan *et al.* 2021). Herein we quantify the Si burial by diatom populations over multiple years. This novel ability enables us to enumerate the influence that community turnover will have upon the silica cycle. It is currently typical for paleolimnologists to express changes in diatom communities as either percent or actual abundance and use those data as proxies for paleoenvironments (Julius & Theriot 2010). We offer a direct measure of the influence a species has upon nutrient cycles. In this case we quantify the amount of Si buried by *S. niagarae* each year.

El Niño 3.4 has an effect size on summer precipitation of 0.05 standard deviations which is both indirect of *S. niagarae* Si mass and of extremely small effect size and could not be dissected from other causes of change in *S. niagarae* Si mass in a paleontological study. *S.*

niagarae Si mass is not likely to be used as a proxy for ENSO in this region (Table 4.1 & Fig. 4.4). Likewise PDO and the PDSI are not correlated to any of the novel proxies described herein as neither climate index showed correlation of the data.

Limitations of the method

Transferability of the FlowCAM automated measuring approach is currently limited by the ability of automated imaging to correctly identify species. While analyzing the Herd Lake archive the major taxa were possible to delineate because of the low diversity. There were only two major plankton. *S. niagarae* and *S. parvus* together comprised over 95-99% of the diatom community in each sample. *S. niagarae* was easily recognized via sorting algorithm based on size and aspect ratio alone. *S. parvus* proved too small to be parsed out accurately from other small particles. Integrating deep learning approaches to automated diatom identification may overcome the barriers presented by more diverse diatom communities (Pedraza *et al.* 2017).

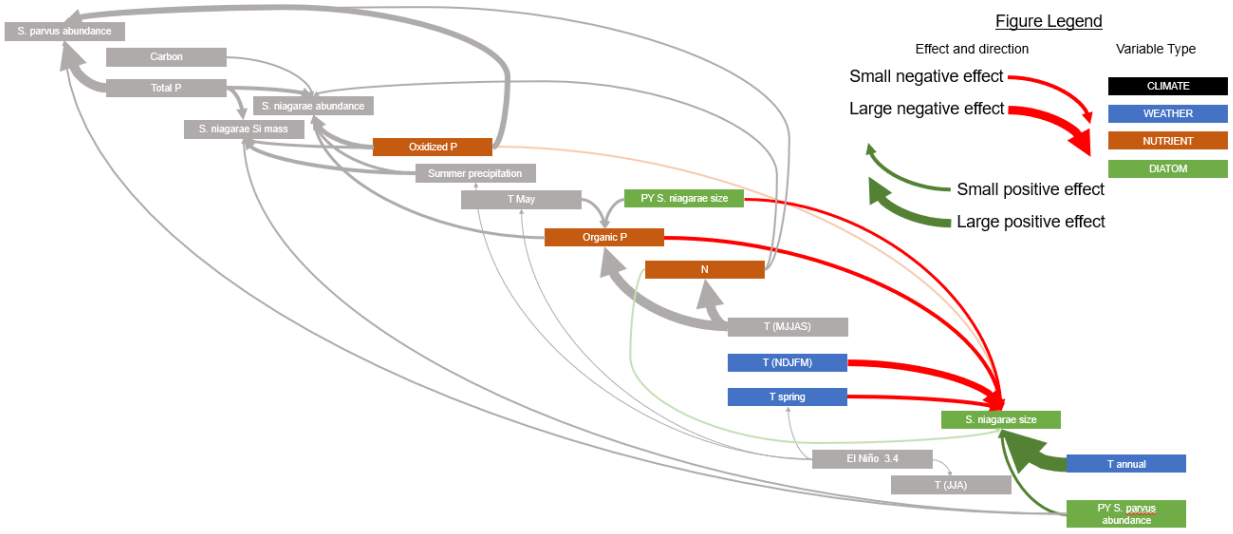

Figure 4.5 Results from the structural equation model highlighting the variables that exert pressures on the size of *S. niagarae*.

We were also only able to calculate the Si volume of *S. niagarae* because previous studies had already created accurate measures of the Si volume across the entire size range of the species (Mohan *et al.* 2021). Currently *S. niagarae* is the only species with such a formula calculated to derive 3D Si volume from size measurements of 2D images. This may be overcome by creating a 3D modeling library of diatom species so that Si volume data becomes readily and publicly accessible.

There are several interesting observations from our results. Many external variables influence the average diameter of a *S. niagarae* population. Warmer years are associated with increases in cell size, while colder winters and springs result in smaller size *S. niagarae*. Diatoms regain their maximum size through sexual reproduction and diminish in size via asexual reproduction (Lewis 1984). Hence, we suggest that lake conditions that result from warmer annual temperatures favor sexual reproduction in *S. niagarae,* while conditions that result from colder or longer winters favor asexual reproduction. Further, summer temperature does not directly affect the size of *S. niagarae* and suggests that sexual reproduction is probably associated with length of summer stratification period rather than temperature directly. We observe that higher organic phosphorus reduces the size of *S. niagarae* which is likely driven by increased asexual reproduction because diatom populations shrink in diameter under asexual reproduction.

Because we are dealing with buried sediment, correlations of climate, weather, nutrient, and diatom data are prone to some mechanistic scenarios where these correlations are the result of circular reasoning or are possibly self-referential. *E.g.* if abundance of a diatom species is highly correlated with nitrogen then either the diatom is more abundant during times of high nitrogen or that diatom buries nitrogen at a higher rate. Modern observations or experiments

would be able to parse out the mechanism. The correlations are important to point out because they offer clues and give direction for future experiments that can reveal the mechanism, *e.g.* the diatom species buried more nitrogen or the diatom is more abundant during high nitrogen phases.

Conclusions

The approach that we establish here provides a novel metric for directly measuring the influence that a species of diatoms exerts upon the silica cycle. This novel metric also reveals ecological influences upon a diatom population that are not apparent in abundance, size, or community structure data and are independent of the influence from other nutrients. Expanding this technique to many common species of diatom will allow us to predict changes in global silica cycling that result from climate change and anthropogenically-driven lake trophic level changes via diatom community turnover. We also reveal major drivers of diatom size diminution and regain which highlight the role of external triggers of sexual reproduction in *S. niagarae.*

CHAPTER 5 CONCLUSIONS

This research develops a new way of analyzing phytoplankton and demonstrates two applications of 3D modeling of microscopic organisms. We can more accurately estimate the biovolume of phytoplankton with this method. This method also allows us to place phytoplankton into computer simulation to assess how a single trait can affect sinking behavior of a species. We also have a new way to directly measure the impact that a species has upon nutrient cycles in lakes rather than relying on proxies and transfer functions. These approaches show promise to advance understanding of phytoplankton evolution, ecological impacts, applications for nano-technology, and paleontology.

In Chapter 2, I develop more accurate 3D models of diatoms that differ from previous attempts by up to 20% estimated biovolume. With the development of more 3D models of phytoplankton species, estimates of global phytoplankton primary productivity may become more accurate. The amount of the diatom biovolume that is composed of amorphous silica dioxide is revealed and enables for deciphering species-specific influence on silica cycles in aquatic systems.

In Chapter 3, 3D models of diatoms are placed in computer simulations with modified and unmodified traits to assess the trait function without confounding factors that typically arise from correlated traits in natural specimens. The simulations reveal the resource cost of constructing these traits (spines) out of silica and reveal the benefits received from reduced sinking rate. These benefits cost large diatoms the most resources and large diatoms receive the least benefit whereas the smaller diatoms in a population receive the most benefit and the silica cost is the least in terms of total silica spent on spine construction.

Chapter 4 examines weather, climate, nutrient, and phytoplankton interactions that rely on the novel metrics developed in Chapter 2. The amount of silica biomass that is buried in lake sediment by *S. niagarae* each year is decreased by excessive total phosphorus and increases with oxidized phosphorus, and summer precipitation. It is weakly increased based on the previous year's abundance of *S. parvus.* El Niño cycles may also play a secondary role in the amount of silica buried by weakly influencing the amount of precipitation in the region over the summer however there is no direct influence on the diatom populations.

In Chapter 4, the controls on the size (diameter) of *S. niagarae* are revealed. Annual temperature is the largest driver that increases *S. niagarae* size. Because diatoms regain their maximum size via sexual reproduction, the diatom sex clock (Lewis 1984) for *S. niagarae* is likely controlled by temperature via changes in thermal structure and timing of different thermal regimes in the lake. We also find that *S. niagarae* decreases its size (asexual reproduction) during years with higher OP, and warmer winter and spring. we find more large diatoms during warmer years and more small diatoms during warmer winter and spring. Because diatoms only increase in size during sexual reproduction, we suggest that sexual reproduction occurs more frequently during long warm summers.

Synthesizing the methods from chapter 2 that find the volume of silica in each diatom with the population dynamics in chapter 4 we find discrepancies in current estimated biovolume of populations of algae. Using a cylindrical model to find the biovolume of a population (Sun & Liu 2003) over estimates the population's biovolume compared to the method described in chapter 2 (Mohan *et al.* 2021) especially when applied to the larger diameter diatoms. This

suggests that there is much improvement to be made in assessing biovolume of algae and understanding how algae influence nutrient pools and cycles.

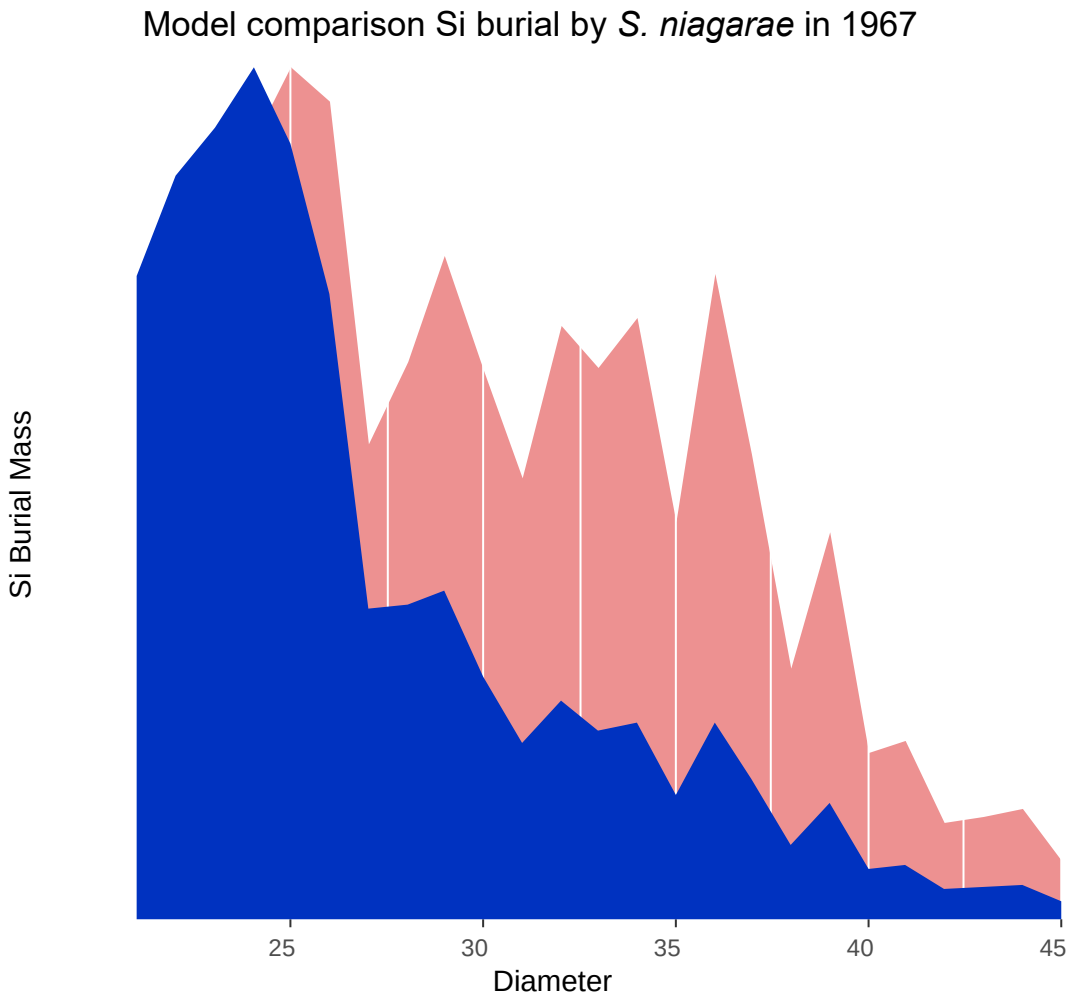

Figure 5.1: comparison of biovolume estimates of a population of *S. niagarae* from the Herd Lake sediment core from the varve layer buried in 1967. Red indicated biovolume estimate of this population using the cylindrical method proposed by Sun *et al* (2003). Blue indicated the biovolume estimates derived from the methods developed in chapter 2 of this dissertation (Mohan *et al* 2021)

The next questions to pursue in this line of research are numerous. The tools available to analyze 3D models are a vast and rapidly growing field. Promising areas of research for ecological applications are to expand the number of accurate models of phytoplankton species. Maintaining a digital archive of 3D diatom models would enable researchers, teacher, policy makes, and water quality monitors to explore influences that each diatom species have on nutrient cycles. 3D models of diatoms have been used in nano-technology; this field would also be greatly enhanced if more 3D models species of diatom were readily available in a digital archive. In the field of evolutionary biology these 3D methods are likely to reveal trait functional pressures that phenotypic changes have on sinking behavior and evolution of diatoms. Specifically, I would ask how does the evolution of spine distribution affect the cost benefit ratio of a diatom species that evolves rapidly and has morphologically similar related species (*S. niagarae, S. yellowstonensis, S. superiorensis, S. reimeri*).

REFERENCES

Anderson, L.D. & Delaney, M.L. (2000) Sequential extraction and analysis of Phosphorus in marine sediments: streamlining of the SEDEX procedure. *Limnology and Oceanography* 45, 509–515.

Batchelor, G.K. (2000) Flow of a Uniform Incompressable Viscous Fluid. In: *An Introduction to Fluid Dynamics*. Cambridge University Press, Cambridge, pp. 174–263.

Battarbee, R.W., Jones, V.J., Flower, R.J., Cameron, N.G., Bennion, H., Carvalho, L. & Juggins, S. (2001) 3 Tracking Environmental Change Using Lake Sediments *Diatoms*. J. P. Smol, H. J. B. Birks, and W. M. Last (Eds). Dordrecht, Netherlands.

Bienfang, P.K., Harrison, P.J. & Quarmby, L.M. (1982) Sinking rate response to depletion of nitrate, phosphate and silicate in four marine diatoms. *Marine Biology* 67, 295–302.

Box, G.E.P. (1976) Science and Statistics. *Journal of the American Statistical Association* 71, 791–799.

Boyce, D.G., Lewis, M.R. & Worm, B. (2010) Does blending of chlorophyll data bias temporal trend ? *Nature* 466, 591–596.

Capriulo, G.M. & Carpenter, E.J. (1980) Grazing by 35 to 202 um microzooplankton in Long Island Sound. *Marine Biology* 56, 319–326.

Cohen, M.J., Creed, I.F., Alexander, L., Basu, N.B. & Calhoun, A.J.K. (2016) Do geographically isolated wetlands influence landscape functions ? 113, 1978–1986.

Conley, D.J., Kilham, S.S. & Theriot, E. (1989) Differences in silica content between marine and freshwater diatoms. *Limnology and Oceanography* 34, 205–213.

Demaster, D.J. (1981) The supply and accumulation of silica in the marine environment. *Geochemica et Cosmochimica Acta* 45, 1715–1732.

Fathi, H. & Lourakis, M. (2015) Automated as-built 3D reconstuction of civil infrastructure using computer vision: Acheivements, opportunities, and challenges. *Advanced Engineering Informatics* 29, 149–161.

Ferris, J.A. & Lehman, J.T. (2007) Interannual variation in diatom bloom dynamics: Roles of hydrology, nutrient limitation, sinking, and whole lake manipulation. *Water Research* 41, 2551–2562.

Frings, P.J., Clymans, W., Jeppesen, E., Lauridsen, T.L., Struyf, E. & Conley, D.J. (2014) Lack of steady-state in the global biogeochemical Si cycle: emerging evidence from lake Si sequestration. *Biogeochemistry*.

Gifford, D.J., Bohrer, N. & Boyd, C.M. (1981) Spines on diatoms : Do copepods care? *Limnology and Oceanography* 26, 1057–1061.

Guasto, J.S., Rusconi, R. & Stocker, R. (2012) Fluid Mechanics of Planktonic Microorganisms.

Häkansson, H. (2002) A Compilation and Evaluation of Species in the General Stephanodiscus, Cyclostephanos and Cyclotella With a New Genus in the Family Stephanodiscaceae. *Diatom Research* 17, 1–139.

Håkansson, H. & Theriot, E.C. (1984) Observations on the type material of Stephanodiscus hantzschii Grunow in Cleve & Grunow. *Nova Hedwigia* 39, 477–495.

Hamade, R.F., Artail, H.A. & Jaber, M.Y. (2007) Evaluating the learning process of mechanical CAD students. *Computers and Education* 49, 640–661.

Harrison, J.A., Frings, P.J., Beusen, A.H.W., Conley, D.J. & McCrackin, M.L. (2012) Global importance, patterns, and controls of dissolved silica retention in lakes and reservoirs. *Global Biogeochemical Cycles* 26, 1–12.

Harshburger, B., Ye, H. & Dzialoski, J. (2002) Observational evidence of the influence of Pacific SSTs on winter precipitation and spring stream discharge in Idaho. *Journal of Hydrology* 264, 157–169.

Harwood, D.M. (2010) Diatomite. In: J. P. Smol and E. F. Stoermer (Eds), *The diatoms: applications for the environmental and earth sciences*. Cambridge University Press, Cambridge, UK, pp. 570–574.

Hillebrand, H., Durselen, C.-D., Kirschtel, D., Pollingher, U. & Zohary, T. (1999) Biovolume calculation for pelagic and benthic microalgae. *Journal of Phycology* 35, 403–424.

Hofmann, A., Roussy, D. & Filella, M. (2002) Dissolved silica budget in the North basin of Lake Lugano. *Chemical Geology* 182, 35–55.

Interlandi, S.J., Kilham, S.S., Ecology, S. & May, N. (2001) Limiting Resources and the Regulation of Diversity in Phytoplankton Communities. *Ecology* 82, 1270–1282.

Interlandi, S.J., Kilham, S.S. & Theriot, E.C. (1999) Responses of phytoplankton to varied resource availability in large lakes of the Greater Yellowstone Ecosystem. *Limnology and Oceanography* 44, 668–682.

Interlandi, S.J., Kilham, S.S. & Theriot, E.C. (2003) Diatom– chemistry relationships in Yellowstone Lake (Wyoming) sediments: Implications for climatic and aquatic processes research. *Limnology and Oceanography* 48, 79–92.

Julius, M.L. & Theriot, E.C. (2010) The diatoms: a primer. In: *The diatoms: applications for the environmental and earth sciences*. , pp. 8–22.

Kilham, S.S., Theriot, E.C. & Fritz, S. (1996) Linking planktonic diatoms and climate change in the large lakes of the Yellowstone ecosystem using resource theory. *Papers in the Earth and Atmospheric Sciences* 41, 1052–1062.

Kingsolver, J.G., Gomulkiewicz, R. & Carter, P.A. (2001) Variation , selection and evolution of function-valued traits. , 87–104.

Kovala, P.E. & Larrance, J.P. (1966) Computation of Phytoplankton Cell Numbers, Cell Volume, Cell Surface Area and Plasma Volume per Litre, from Microscopical Counts. *Special Report University of Washington, Seattle, WA* 38, 1–91.

Krebs, W.N., Bradbury, J.P. & Theriot, E.C. (1987) Neogene and Quaternary Lacustrine Diatom Biochronology, Western USA. *Palaios* 2, 505–513.

Kruse, S., Jansen, S., Krägefsky, S. & Kruse, U.B. (2009) Gut content analyses of three dominant Antarctic copepod species during an induced phytoplankton bloom EIFEX (European iron fertilization experiment). *Marine Ecology* 30, 301–312.

Lande, R. & Arnold, S.J. (1983) The Measurement of Selection on Correlated Characters. *Evolution* 37, 1210–1226.

Lewis, W.M.J. (1984) The diatom sex clock and its evolutionary significance. *The American Naturalist* 123, 73–80.

Liu, D., Yuan, P., Tian, Q., Liu, H., Deng, L., Song, Y., Zhou, J., Losic, D., Zhou, J., Song, H., Guo, H. & Fan, W. (2019) Lake sedimentary biogenic silica from diatoms constitutes a significant global sink for aluminium Dong. *Nature Communications* 10, 1–7.

Livingstone, D.A. (1955) A lightweight piston sampler for lake deposits. *Ecology* 36, 137–139.

Loucaides, S., Van Cappellen, P., Roubeix, V., Moriceau, B. & Ragueneau, O. (2011) Controls on the Recycling and Preservation of Biogenic Silica from Biomineralization to Burial. *Silicon*.

Lu, J., Sun, C. & Wang, J. (2015) Mechanical Simulation of a Diatom Frustule Structure. *Journal of Bionic Engineering* 12, 98–108.

Lurling, M. (2021) Grazing resistance in phytoplankton. *Hydrobiologia* 848, 237–249.

McQuatters-Gollop, A., Reid, P., Edwards, M., Burkhill, P.H., Castellani, C., Batten, S., Geiskes, W., Beare, D., Bidigare, R.R., Head, E., Johnson, R., Kahru, M., Koslow, J.A. & Pena, A. (2011) Is there a decline in marine phytoplankton? *Nature* 472, E6–E7.

Mohan, J., Saros, J. & Stone, J.R. (2021) On the matter of phytoplankton : A novel method using 3D computer models to calculate biovolume of microorganisms.

Mullin, M.M., Sloan, P.R. & Eppley, R.W. (1966) Relationship between carbon content, cell volume, and area in phytoplankton. *Limnology and Oceanography*, 307–311.

Myrbo, A. & Wright, H.E. (2008) An introduction to Livingstone and Bolivia coring equipment. *Limnological Research Center Core Facilit SOP Series:* Available from: http://lrc.geo.umn.edu/laccore/assets/pdf/sops/livingstone-bolivia.pdf.

Nguyen, H., Karp-boss, L., Jumars, P.A. & Fauci, L. (2011) Hydrodynamic effects of spines : A different spin. *Limnology and Oceanography: Fluids and Environments* 1, 110–119.

Nymark, M., Sharma, A.K., Sparstad, T., Bones, A.M. & Winge, P. (2016) A CRISPR / Cas9 system adapted for gene editing in marine algae. *Scientific Reports*, 6–11.

Paasche, E. (1960) On the relationship between primary production and standing stock of phytoplankton. *J. Conseil Perm. Internation Exploration Mer.* 26, 33–48.

Pancic´, M., Torres, R.R., Almeda, R. & Kiørboe, T. (2019) Silicified cell walls as a defensive trait in diatoms. *Proceedings of the Royal Society B* 286, 1–8.

Pedraza, A., Bueno, G., Deniz, O., Cristóbal, G., Blanco, S. & Borrego-Ramos, M. (2017) Automated Diatom Classification (Part B): A Deep Learning Approach. *Applied Science* 7, 1–25.

Price, T. & Langen, T. (1992) Evolution of Correlated Characters. *TREE* 7, 307–310.

Purcell, E.M. (1977) Life at low reynolds number. *American Journal of Physics* 45, 3–11.

R Core Team (2020) R: A language and environment for statistical computing.

Raven, J.A. & Waite, A.M. (2004) The evolution of silicification in diatoms: Inescapable sinking and sinking as escape? *New Phytologist* 162, 45–61.

Reynolds, C.S. & Wiseman, S.W. (1982) Sinking losses of phytoplankton in closed limnetic systems. *Journal of Plankton Research* 4, 489–522.

Rocha, C.D. La (2002) Tracing the silica cycle with silicon isotopes. *Série de documents océanographiques, Institut Océanographique* 28, 369–382.

Rossel, Y. (2012) lavaan: An R Package for Structural Equation Modeling. *Journal of Statistical Software* 48, 1–36.

Ruttenberg, K.C. (1992) Development of a sequential extraction method for different forms of phosphorus in marine sediments. *Limnology and Oceanography* 37, 1460–1482.

Saros, J.E. & Anderson, N.J. (2015) The ecology of the planktonic diatom Cyclotella and its implications for global environmental change studies. *Biological Reviews* 90, 522–541.

Saros, J.E., Stone, J.R., Pederson, G.T., Slemmons, K.E.H., Spanbauer, T., Schliep, A., Cahl, D., Williamson, C.E. & Engstrom, D.R. (2012) Climate-induced changes in lake ecosystem structure inferred from coupled neo- and paleoecological approaches. *Ecology* 93, 2155–2164.

Schmid, A.M., Borowitzka, M.A. & Volcani, B.E. (1981) Morphogenisis and Biochemistry of Diatom Cell Walls. In: O. Kiermayer (Ed), *Cytomorphogenesis in Plants. Cell Biology Monographs, vol 8*. Springer, Vienna.

Shapley, M.D., Finney, B.P. & Krueger, C.R. (2019) Characteristics of landslide-formed lakes of central Idaho : High-resolution archives of watershed productivity and clastic sediment delivery. *Geologic Society of America* Special Pa, 241–258.

Sicko-Goad, L.M., Schelske, C.L. & Stoermer, E.F. (1984) Estimation of intracellular carbon and silica content of diatoms from natural assemblages using morphometric techniques. *Limnology and Oceanography* 29, 1170–1178.

Sicko-Goad, L.M., Stoermer, E.F. & Ladewski, B.G. (1977) A Morphometric Method for Correcting Phytoplankton Cell Volume Estimates. *Protoplasma* 93, 147–163.

Smayda, T.J. (1970) The suspension and sinking of phytoplankton in the sea. *Marine Biology* 8, 353–414.

Smetacek, V.S. (1985) Role of sinking in diatom life-history cycles : ecological , evolutionary and geological significance. *Marine Biology* 84, 239–251.

Smith, C. (2018) Niño 3.4 SST Index. Available from: https://psl.noaa.gov/gcos_wgsp/Timeseries/Nino34/.

Smol, J.P. & Stoermer, E.F. (2010) Applications and uses of diatoms: plologue. In: J. P. Smol and E. F. Stoermer (Eds), *The diatoms: applications for the environmental and earth sciences*. Cambridge University Press, Cambridge, UK, pp. 3–7.

Steilein, A. (1996) Utilization of CAD models for the object oriented measurement of industrial and architectural ogjects. *International Archives of Photogrammetry and Remote Sensing* 21, 548–553.

Stone, J.R., Saros, J.E. & Pederson, G.T. (2016) Coherent late-Holocene climate-driven shifts in the structure of three Rocky Mountain lakes. *The Holocene*, 1–9.

Strathmann, R.R. (1967) Estimating the organic content of phytoplankton from cell volume or plasma volume. *Limnology and Oceanography*, 411–418.

Strickland, J.D.H. & Parsons, T.R. (1972) A Practical Handbook of Seawater Analysis 2nd ed. *Bulletin, Fisheries Research Board of Canada* 167.

Sun, J. & Liu, D. (2003) Geometric models for calculating cell biovolume and surface area for phytoplankton. *Journal of Plankton Research* 25, 1331–1346.

Tetzlaff, D., Soulsby, C., Bacon, P.J. & Youngson, A.F. (2007) Connectivity between landscapes and riverscapes — a unifying theme in integrating hydrology and ecology in catchment science ? 1389, 1385–1389.

Theriot, E. (1987) Principal component analysis and taxonomic interpretation of environmentally related variation in silicification in Stephanodiscus (Bacillariophyceae). *British Phycological Journal* 22, 359–373.

Theriot, E. & Bradbury, J.P. (1987) Mesodictyon, a new fossil genus of the centric diatom family Thalassiosiraceae from the Miocene Chalk Hills Formation, western Snake River Plain, Idaho. *Micropaleontology* 33, 356–367.

Theriot, E.C., Fritz, S.C., Whitlock, C. & Conley, D.J. (2006) Late Quaternary rapid morphological evolution of an endemic diatom in Yellowstone Lake, Wyoming. *Paleobiology* 32, 38–54.

Theriot, E.C. & Stoermer, E.F. (1982) Observations on North American Populations of Stephanodiscus (Bacillariophyceae) Species Attributed to Friedrich Hustedt. *Transactions of the American Microscopical Society* 101, 368–374.

Theriot, E.C. & Stoermer, E.F. (1984) Principal Component Analysis of Stephanodiscus Observations on Two New Species from the Stephanodiscus niagarae. *Bacillaria* 7, 37–53.

Tréguer, P., Bowler, C., Moriceau, B., Dutkiewicz, S., Gehlen, M., Aumont, O., Bittner, L., Dugdale, R., Finkel, Z., Iudicone, D., Jahn, O., Guidi, L., Lasbleiz, M., Leblanc, K., Levy, M. & Pondaven, P. (2018) Influence of diatom diversity on the ocean biological carbon pump. *Nature Geoscience* 11, 27–37.

Tréguer, P., Nelson, D.M., Bennekom, A.J. Van, Demaster, D.J. & Quéguiner, B. (1995) The Silica Balance in the World Ocean : A Reestimate Published by : American Association for the Advancement of Science Stable URL : http://www.jstor.org/stable/2886587. 268, 375–379.

Treguer, P.J. & De La Rocha, C. (2013) The World Ocean Silica Cycle. *Annual Review of Marine Science*, 5, 477–501.

Tuchman, B.M.L., Theriot, E. & Stoermer, E.F. (1984) Effects of Low Level Salinity Concentrations on the Growth of Cyclotella meneghiniana KUTZ . (Bacillariophyta). *Archiv für Protistekunde* 128, 319–326.

Waite, A., Fisher, A., Thompson, P.A. & Harrison, P.J. (1997) Sinking rate versus cell volume relationships illuminate sinking rate control mechanisms in marine diatoms. *Marine Ecological Progress Series* 157, 97–108.

Walker, J.A. (2014) THE EFFECT OF UNMEASURED CONFOUNDERS ON THE ABILITY TO ESTIMATE A TRUE PERFORMANCE OR SELECTION GRADIENT (AND OTHER PARTIAL REGRESSION THE EFFECT OF UNMEASURED CONFOUNDERS ON THE ABILITY TO ESTIMATE A TRUE (AND OTHER PARTIAL REGRESSION COEFFICIENTS). *Evolution* 68, 2128–2136.

Willén, E. (1976) A simplified method of phytoplankton counting. *British Phycological Journal* 11, 265–278.

Wolfe, A.P., Hobbs, W.O., Birks, H.H., Briner, J.P., Holmgren, S.U., Ingólfsson, Ó., Kaushal, S.S., Miller, G.H., Pagani, M., Saros, J.E. & Vinebrooke, R.D. (2013) Stratigraphic expressions of the Holocene-Anthropocene transition revealed in sediments from remote lakes. *Earth-Science Reviews* 116, 17–34.

APPENDIX SUPPLAMENTAL TEXT AND FIGURE FOR CHAPTER 1

Expanded methods for diatoms

Herd Lake, Idaho, USA (44°05'21.9"N, 114°10'26.1"W) contains a well-preserved diatom archive that is primarily comprised of two species, *S niagarae* and *S parvus.* The core recovered from the central deep basin of Herd Lake exhibits varves for the past ~1700 years continually (Shapley *et al.* 2019). The varve couplets are ~ 1 cm thick and were subsampled at yearly increments. Years with concentrations of *S niagarae* over 50% were used for this study and contained 45,000 – 11,000,000 valves per gram (Mohan, *unpublished data*). These sub-samples were selected for an abundance of valves to ensure data collection across the size range of this population.

Light microscopy was conducted on a Leica DM-2500 light microscope under 1000x magnification. Light microscopy was conducted to determine the proportion of spines, costae, rimoportulae, and mantle height to the diameter of each valve. The number of spines, costae, and rimoportulae were counted on 248 valves which range in diameter 39 – 70 μm. Mantle height was measured on 45 valves with a range of 38 – 76 μm (Figure A.1). Following Theriot and Stoermer (1984) & Theriot et al. (2006) we noted that in the *S. niagarae* spines are always associated with a co-occurring mantle fultoportulae. The Herd Lake specimens exhibit this relationship, thus counts for mantle fultoportulae herein are derived from spine counts.

Scanning electron micrographs were created via a Vega II scanning electron microscope. Scanning electron microscopy was conducted to determine the proportion of areolae per fascicle, central fultoportulae, and valve thickness to diameter. Scanning electron microscopy also provided dimensions of each ultrastructure included in the 3D-model. The number of areolae in at least 10 fascicles per valve were counted for 34 valves ranging in diameter from 38 – 64 μm.

Central fultoportulae were counted on 29 valves with a range of 41 – 58 µm. The thickness of the basal siliceous disc (valve thickness) was measured in 58 valves which ranged in diameter 35 – 65 µm (Figure A.1).

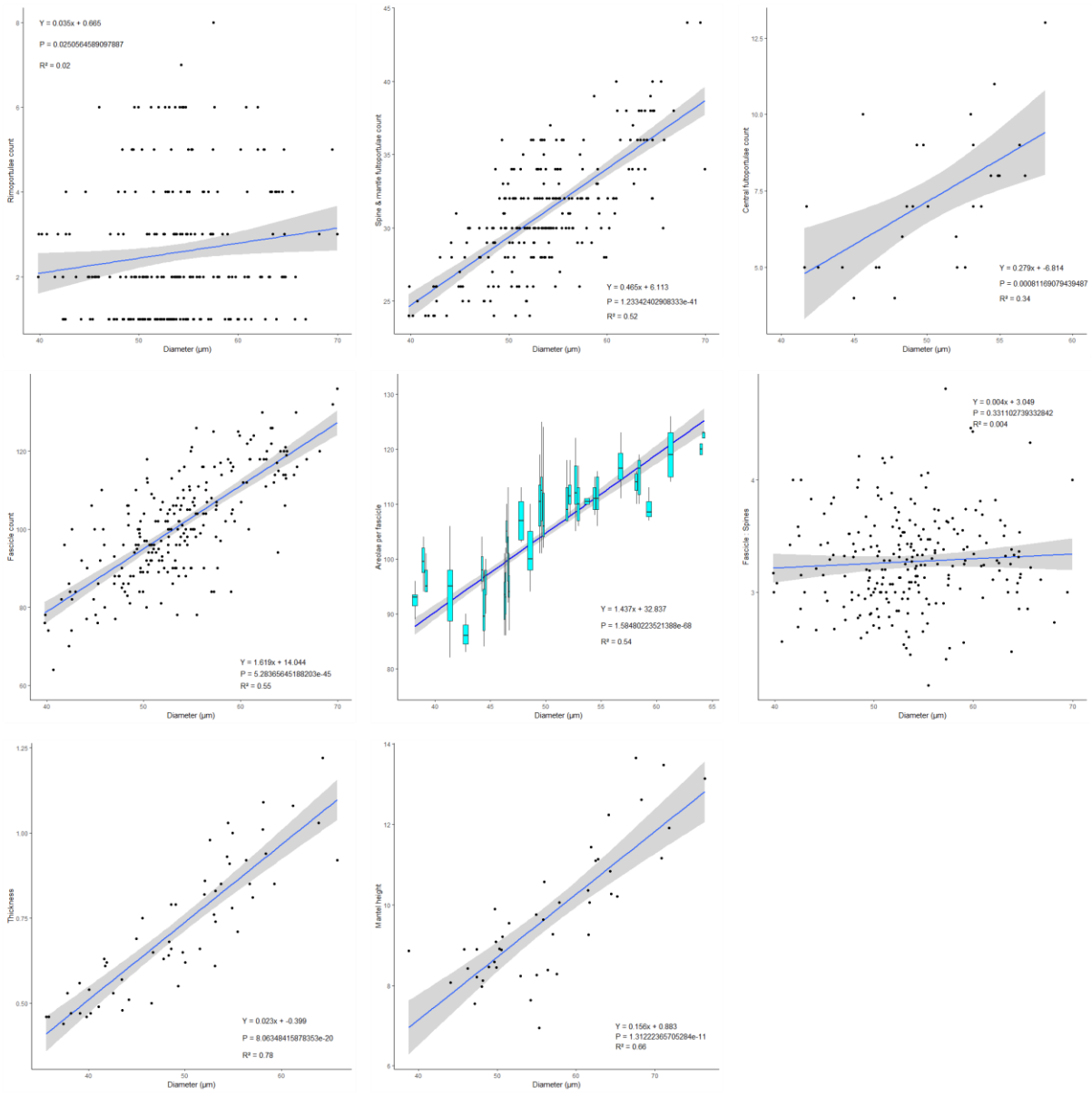

Figure A.1 Distribution of components that make up the diatom valve

Expanded discussion for diatoms

To address the volume of cingulum (girdle bands). The girdle bands are simple structures that probably do not warrant 3D modeling for most species as their volume can be calculated by multiplying the surface area of a 2d projection of the mantle perimeter by the height and subtracting a the same of a slightly smaller 2d projection. For a circular diatom this would equate to the volume of a tube ~.5 μm thick. Thus *S. niagarae* from this study would have a range in girdle band volume $541^{\mu m3}$ – $1170^{\mu m3}$. Some diatom species will have other structures and more intricate girdle bands such as ligula which overlap the split in a band next to it. Septa may also pose issues for taxa that have valvocopula *e.g. Tabellaria* and *Teracyclus* which may represent a significant portion of the silica sink.

Diameter	Mantle height	Valve thickness	Spines	Mantle Fultoportulae	Central Fultoportulae	Rimoportulae	Areolae per fascicle	Fascicles (Costae)	total areolae
75.0000	12.5830	1.3260	41	41	14	3	141	135	19049
70.0000	11.8030	1.2110	39	39	13	3	133	127	16995
65.0000	11.0230	1.0960	36	36	11	3	126	119	15058
60.0000	10.2430	0.9810	34	34	10	3	119	111	13237
55.0000	9.4630	0.8660	32	32	9	3	112	103	11533
50.0000	8.6830	0.7510	29	29	7	2	105	95	9945
45.0000	7.9030	0.6360	27	27	6	2	98	87	8473
40.0000	7.1230	0.5210	25	25	4	2	90	79	7117
35.0000	6.3430	0.4060	22	22	3	2	83	71	5878

Table A.1 Average height, thickness, and number of each component used to construct the nine representative 3D CAD models

These models of *S. niagarae* include the rimoportulae and fultoportulae as having their true hollow tube design however if future studies are short on time, these features constitute less than one percent of the total volume and inclusion or exclusion of the hollow tube feature is unlikely to distort results significantly. Other hollow structures within diatoms are vacuoles that may constitute up to 40% of the diatom volume. Species that contain vacuoles may be corrected for vacuolar space by integrating vacuoles into the 3D models or by following other morphometric methods (*e.g.* Sicko-Goad et al. 1977).

A confounding variable for the implementation of this method to ecological and paleontological studies is that diatoms can vary the degree of silicification in their valves based upon environmental stressors. Theriot (1987) found that degree of silicification varies with the Si : P of the environment while Si alone did not have a significant effect on silicification. Salinity and growth rate also play a roll in valve silicification highlighted by differences between marine and freshwater taxa (*e.g.* Håkansson and Theriot 1984;Tuchman et al. 1984; Conley et al. 1989).

BIOGRAPHY OF THE AUTHOR

Joseph Mohan was born and raised in Michigan. He graduated from Salem High School in 2009. Attended Central Michigan University and graduated in 2014 with a B.S. in Geology. Went on to Indiana State University and graduated in 2017 with a Masters in Earth Science. Joined the University of Maine in the Ecology and Environmental Science program as well as the Climate Change Institute. After receiving his degree, he hopes to live happily ever after with his wife, dog, and anyone else that joins the family. He will also be a post-doctoral research fellow at the St. Croix Watershed Research Station. Joseph is a candidate for the Doctor of Philosophy degree in Ecology and Environmental Science from the University of Maine in May 2022.